UNIVERSITÀ DEGLI STUDI DI MILANO
FACOLTÀ DI MEDICINA E CHIRURGIA

DIPARTIMENTO DI FISICA "ALDO PONTREMOLI"

Scuola di Specializzazione in
Fisica Medica

DOSIMETRY PREDICTORS OF LATE AND ACUTE TOXICITY AFTER WHOLE BREAST RADIOTHERAPY IN A MONOINSTITUTIONAL LARGE POPULATION

Supervisor: Prof.ssa Cristina Lenardi
Co-Supervisors: Dr C. Fiorino, Dr T. Rancati
Outside Examiner: Dr M. Avanzo, Dr V. Landoni

Candidate:
Alessandro Cicchetti
Serial. Nr. S63354

Academic year 2020-2021

"Recuerdo más
de lo que he visto"

– Vitalic

Abstract

The thesis study aimed to identify dosimetric NTCP models for acute and late skin toxicity after breast cancer radiotherapy. The investigated cohort consisted of 1325 early-stage breast cancer patients treated at San Raffaele Hospital between 2009 and 2017 with a hypofractionated scheme (40 Gy in 15 fractions) without boost delivered to the whole breast. To explore the possible causality between the damage to the cutaneous tissue and the acute and late reactions, we focused on the dose distribution of the skin, defined as the first 5 mm body layers. The study endpoints were: (i) any acute grade 2 or plus skin toxicity; (ii) oedema and hyperpigmentation development; (iii) late moderate/severe grade of fibrosis, atrophy, telangiectasia and pain; and (iv) liponecrosis. For the first time in these endpoints, the considered Organ at Risk for the dosimetry was the first 5 mm of the breast skin. The PTV volume was confirmed as one of the most impacting factors in developing any sequela (except liponecrosis). The volume receiving 20 Gy, the 50% of the prescription dose, was applied as a dosimetric descriptor in models for (i), (ii), (iii) and was able to replace PTV giving, at the same time, the possibility to better interpret the damage in terms of irradiated skin as well as being more generalizable, being independent on the contouring phase; in addition, V42 Gy was entered in the model for describing late toxicity (iii). Among the treatment and patient factors, lymph node dissection was the most impacting factor for three of the four endpoints (i-ii-iii), and it was included as a covariate in the model together with the dosimetric descriptor. Obesity was identified as a risk factor for early skin reaction, while aromatase inhibitor and hormone therapy and age were found as protective factors in a multivariate model for late toxicity and liponecrosis, respectively. The cosmetic status after surgery was found to be associated with the development of late fibrosis and was included in that multivariable model to account for the damage to the breast parenchymal tissue caused by the conservative surgery.

Contents

Chapter 1

Introduction

The global incidence of breast cancer has been rising with an annual increase of 3.1%, beginning with 641.000 cases in 1980 and reaching 2.1 million women with a new diagnosis in 2018. The trend is likely to continue caused of population growth, ageing and the increasing access to improved diagnostic techniques for early detection in developing countries [37]. Currently, more than 70% of breast cancer (BCa) patients undergo adjuvant radiotherapy following surgery. Decades of investigations through multiple prospective randomized trials at the end of the century led to relevant improvement in disease survival, with limited side effects. Nowadays, the ten-year survival rate exceeds 80% in the early stage BCas, while it was 65% for women with pathologically verified nodal status [70, 36].

1.1 RT options in the management of early-stage BCa

Since the last decades of the past century, breast-conserving surgery (BCS) was demonstrated to be equivalent to mastectomy in terms of local control and overall survival [81] but with a positive and reported effect on the cosmetic and patients' quality of life (QoL) [24]. Then, many studies [36, 71] largely demonstrated the positive contribution of radiotherapy following BCS in reducing recurrences and cancer-related death. A comprehensive survey of these results was reported by Darby and colleagues in 2011, considering 10 and 15 years of follow-up (FU) for the two endpoints, respectively. Due to this strong evidence, adjuvant radiotherapy of early breast cancer, with whole breast irradiation (WBI), still represents a significant fraction of radiotherapy treatments delivered worldwide. At the time of this review, all the analyzed trials used conventional fractionation, typically delivering 50 Gy in 25 fractions, which was considered a standard for many years.

Based on radiobiology considerations and the impact on the occupancy of radiotherapy department, adjuvant BCa RT was one of the elective districts to explore the efficacy of hypofractionation (HF) schemes to drastically reduce the treatment duration. Three prospective randomized trials[85, 38, 79] tested the long-term outcomes by comparing the standard WBI against the HF WBI delivered in 3-4 weeks. The findings highlighted the non-superiority of the conventional scheme in terms of local relapses and cancer-specific mortality, with comparable toxicity rates. Due to this, prescription doses between 40 and 42.5 Gy in 15-16 fractions are currently the standard of care for managing early-stage breast cancer patients.

Adding an extra radiation dose is recommended for some clinical indications to reduce the risk of local recurrence. The radiation boost includes one or more extra treatments targeted at the tumour bed, a small area of breast tissue where the original cancer was removed. Surgeons usually mark this area with surgical clips (made out of titanium) that remain in the body to deliver the boost to this critical part. This targeted boost is administered using the same machine used for regular treatments but with lower amounts of radiation than the main course of RT. It can be delivered simultaneously or sequentially to the standard treatment. Moreover, it can be delivered through external (using electrons or photons) or internal RT (Brachytherapy) with a total dose between 4 and 10 Gy.

The American Society for Radiation Oncology (ASTRO) recommends a booster dose for those who meet specific criteria. Primary among them is that breast cancer cells reached the margins, or borders, of the tissue removed during surgery. The radiation boost then offers an added intervention to keep any of these cells from growing. ASTRO recommends a booster dose for patients younger than 50 or older with a high-grade cancer diagnosis. It is not necessary in case of low-intermediate grade with negative margins of more than 2 mm, or for patients older than 70 with positive hormone receptors[74].

Based on a Cochrane review [44], local control appeared to be better with a tumour bed boost. We found no evidence of a difference in overall survival or disease-free survival with or without a tumour bed boost. The percentage of breast retraction assessment did not appear affected by a boost to the tumour bed. Panel-scored cosmesis was significantly better (i.e. good or excellent) if no boost was administered. Physician-scored cosmesis did not differ significantly between groups. Regarding acute radiation dermatitis, there are no differences in the moderate-severe symptoms if the boost is simultaneously or sequentially delivered. A randomized phase 3 trial with 20-year FU showed that the radiation boost after whole-breast irradiation has no effect on long-term overall survival but can improve local control, with the largest absolute benefit in young patients. At the same time, boost increases the risk of moderate to severe fibrosis, but not in the young patients who seem to tolerate the treatment prolongation. Finally, the

extra radiation dose can be avoided in most patients older than 60 years[9]. Dong et al. showed results on the side effects of an HF SIB boost (42.56 – 48 Gy in 16 fr) against a CF sequential boost (25+5 fr) on 185 breast cancer patients[30]. The groups had similar results for late skin toxicity and radiation pneumonitis, while acute skin effects and myelosuppression were lower in the HF arm. Krug and Franceschini reported similar results. In the recent evolution of the radiation schedule (summary in Figure 2 for early BCa, the fast-forward trial investigated a further reduction in the number of fractions with an ultra hypofractionation scheme giving 26 Gy in five fractions (fr) and completing the entire RT in a week. Results at 5 years showed a non-inferiority in ipsilateral tumour relapse and similar skin toxicity or cosmetic impact for patients who underwent 26 Gy in 5 fr [17]. Although health tissue effects continue accumulating over the five years, the relative difference between the arms changes minimally with time, and the results can be interpreted as representative of the long-term condition, although analyses at longer follow-up are still waiting.

As represented in Figure 1, the evolution of breast RT is also following the progression already done by the surgery, with a reduction of the treated volumes, with partial breast irradiation (PBI) as an option for several patients groups through intra-operative radiotherapy, brachytherapy and, more recently, photons and protons IMRT, permitting the delivery of the treatment in few fractions. The delivery of high dose per fraction, close to stereotactic ablative radiation therapy (SABR) exploiting largely available IMRT/VMAT and IGRT technologies is largely preferred, also overcoming the limitations of intra-operative irradiation in the surgical room and the specific skill required for brachytherapy.

Recently, the delivery of a high radiation dose to a limited area covering the tumour core is on the basis of some protocols that aim to prevent the patient's surgery before RT. Such protocols are dedicated to the lowest grade of breast cancer, and patients are then FU frequently in time to guarantee a prompt intervention in case of disease relapse. The IMPORT trial [22] has shown the non-inferiority of the partial breast and reduced-dose RT with similar or fewer late normal-tissue adverse effects for similar patients. This approach gives 40 Gy in 15 fr to the primary target and 36 Gy to the whole breast. Finally, there are protocols that omit the RT and use endocrine therapy as adjuvant treatment for patients with low T stage, tumour size and positive hormone receptors (*ExclUsive endocRine Therapy Or Partial Breast Irradiation for Women Aged* $\leqq$ *70 Years Early Stage Breast Cancer (EUROPA) NCT04134598; EndoNET trial Oxford*).

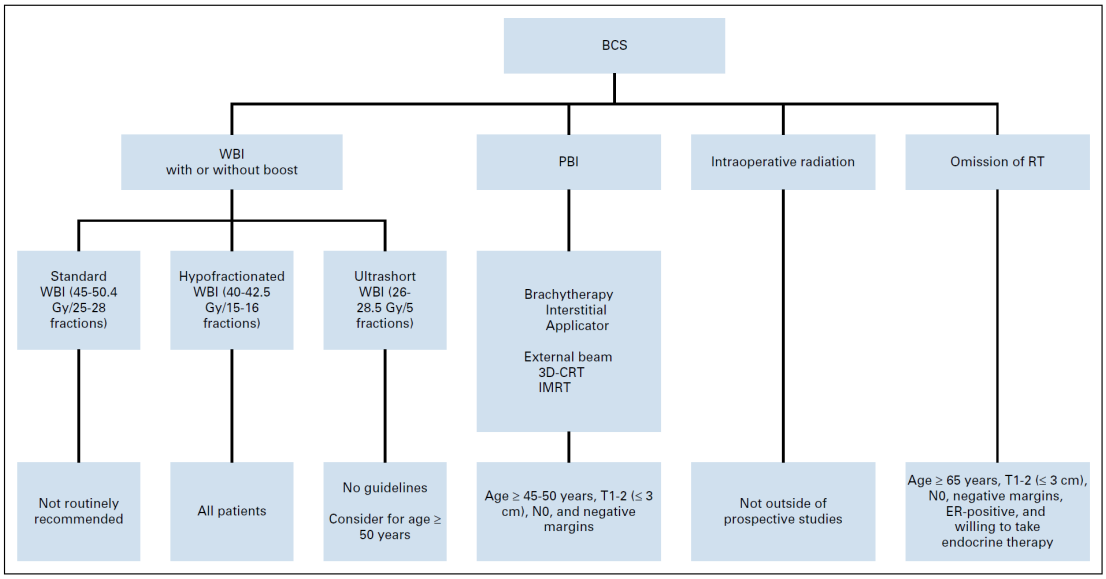

Figure 1: RT options in managing early-stage breast cancer following breast-conserving surgery. 3D-CRT, Three-dimensional conformal radiation therapy, BCS, breast-conserving surgery, ER, estrogen receptor, IMRT, intensity-modulated radiation therapy; PBI, partial breast irradiation; RT, radiation therapy, WBI, whole breast irradiation. Figure extracted from [71]

1.2 RT Techniques

The current practice in WBI generally requires patients in a supine position with the arm well extended above the head, possibly using proper systems assuring a sufficiently comfortable and reproducible setup. Radiation Oncologists delineate the Organs at Risk (OARs) on Computer Tomography (CT) images. Clinical tumour volume (CTV), defined according to national or European guidelines (see ESTRO guidelines REF), includes the whole breast. PTVs are constructed from the CTVs following the institutional CTV-PTV margins and cropped to 5 mm below the skin (the body contour). The ipsilateral lung, the contralateral breast, and the heart are defined as OARs. Photon treatments are delivered with Megavoltage irradiation, generally 6 MV, and using a CT-based treatment planning with isocentric technique. Dose and fractionation schedules can vary based on centre experience and patient characteristics, but the most generalized treatment scheme is 40-42.5 Gy in 15-16 fractions. Dose constraints for the OAR and plan goals for CTV are summarized in Table 1. Electronic portal imaging devices (EPID) and Cone beam CT (CBCT) are among the most used procedures to perform position

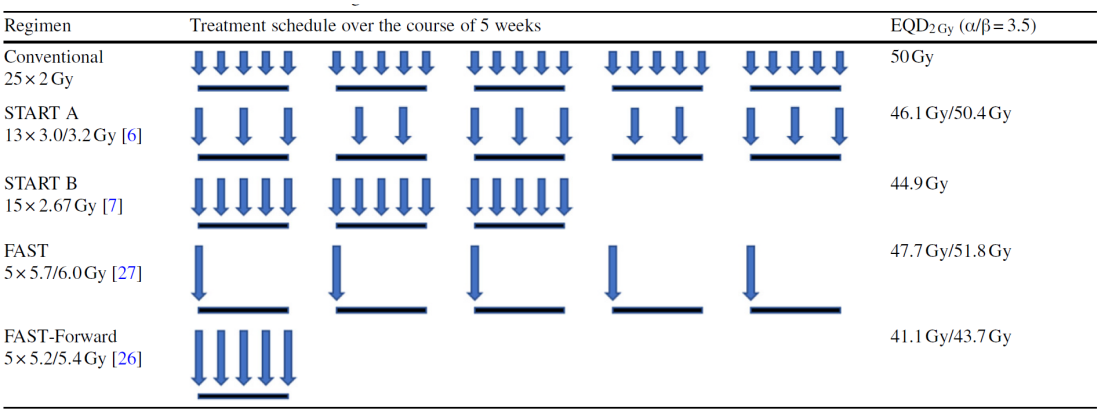

Figure 2: Overview of different fractionation regimens used in clinical trials.Figure extracted from [17]

Table 1: Dose-constraints for whole breast radiotherapy.

CTV (Dose in %)	**Skin Reactions (Dose in %)**	**Ipsilateral Lung (Volume in %)**	**Heart (Gy)**	**Controlateral Breast (Gy)**
Coverage Range 95%-105%	D2% Range 105%-108%	V17 Gy <25%	Mean Dose <2 Gy	Mean Dose <0.5 Gy
Dmax <108%	D2cc <108%	V20 Gy <20%	Dmax <10 Gy	Dmax <5 Gy

verification. External radiation treatments are generally delivered through tangential 3DCRT, forward IMRT using a few segments (field-in-field technique), inverse planned static-field IMRT or inverse planned rotational techniques like Volumetric Modulated Arc Therapy (VMAT) or Helical Tomotherapy.

1.2.1 Traditional 3DCRT with wedges or field-in-field

Advances in computer technology have enabled the possibility of moving from basic 2- dimensional treatment planning and delivery (2D RT) to a more sophisticated approach with 3DCRT thanks to the introduction of CT simulators, TPS for 3D dose calculations, digitally reconstructed radiographs (DRRs), DVHs calculation and MLCs. In 3DCRT, the plans are optimized through manual forward planning, following a trial-and-error approach. The beam angle and the collimator are defined based on the structure contours through the beam's eye view. Mainly, the tangent beams are oriented such that the deep edges of the beams are coplanar (unopposed tangents). Distal gantry angles around 130° and 230° are applied for left and right breast cases; medial angles around 300° and 50° are used for left and right sides. The collimator angle is rotated to account for the curvature of the chest wall minimizing the presence of lung and heart included in the fields.

Consequently, to the beam aperture, an additional margin of about 7 mm needs to be added beyond the PTV in the transverse plane to obtain the desired dose coverage to the PTV. These margins are required to cover the PTV with a minimum isodoses line or surface. Finally, the breast fields have the MLCs open beyond the patients' skin surface to ensure the robustness of the plan in case of swelling and intra-fractional variations. Physical or dynamic wedges are generally used to increase the PTV coverage and the dose distribution homogeneity. Field weights are also adjusted to improve the PTV coverage.

1.2.2 Tangential-like IMRT

A natural evolution of 3DCRT consisted of adding small fields with low weight (5-10% of the main fields) to improve homogeneity. The planner can maintain the same gantry, collimator angle and wedge of the main field to limit the impact on time prolongation. The total number of segments can vary based on the geometrical complexity of the patient's breast. Treatment delivery (including patient setup) typically requires 10-20 minutes. The same approach of using manually optimized multiple segments in a tangential-like approach, often named as "field-in-field" technique, can fully replace wedges and was demonstrated to obtain better results in terms of PTV homogeneity and OARs sparing compared to conventional 3DCRT. The next evolution of FIF is the treatment optimization driven through an inverse planning algorithm and determined by the intensity distributions by an iterative process. The user defines the prescribed dose and dose homogeneity constraints for the PTV and dose-volume constraints for the critical organs. The objective function uses a summation of the squares of the differences between desired and calculated doses in the target and critical organs and user-defined penalties applied to PTV or critical organ points, which violate their constraints. Treatment delivery (including patient setup) required approximately 8–10 min.

1.2.3 Multi-Field IMRT

The ideas of three-dimensionality, beam shaping, and irradiation of tumours through multiple fields from different beam angles to reduce the dose to normal tissues have always been present in radiotherapy practice. Intensity Modulated Radiation Therapy (IMRT) has also been applied to breast cancer as an RT technique to improve uniformity and reduce acute toxicity. Differently from the previous description, multiple static multileaf collimator segments (incrementing by 20-30° the tangential angles) are introduced. The beam parameters for the intensity-modulated fields are the same as those used for the standard plan. The advantages of this approach are evident when 6-8 irradiation fields are designed. The use of sMLC segments resulted in more minor "hot spots" and a lower maximum dose

in the patients while maintaining similar coverage of the treatment volume. On the contrary, the dose bath, i.e. the distribution of low doses far from the target region, increases with this technique.

1.2.4 1.2.4 Volumetric Modulated Arc Therapy

As a natural evolution of IMRT, using the VMAT technique moves the plans toward a more uniform dose in the PTV and to the reduction of the OARs regions receiving high doses next to PTV, especially in the case of concave-shaped PTV. Two (or more) partial continuous arches enrich the possibility of delivering a homogeneous dose to the target reducing the medium-high doses to the OARs. Gantry angles are chosen to force the beam to avoid contralateral beam entries. The skin flash contour is used during optimization to force the MLCs to open beyond the patient contour. During irradiation, position, speed, beam dose rate, and gantry rotation speed on MLC can be modulated to achieve higher target conformity and treatment efficiency. From a technical point of view, VMAT, with non-tangential fields, increases the spread of low doses within the thoracic tissues, the contralateral breast delivery, and more monitor units (MU) per treatment. In clinical practice, the high modulation of this technique is mandatory for PBI, while is highly recommended in multiple isocenter treatments (including bilateral treatment), high fractionation schemes and in patients treated with anthracycline-based chemotherapy. Finally, to mediate between the VMAT advantages and limitations compared to IMRT, non-continuous partial arches are also an option of treatment with a clockwise of 40° per side[82] and in the specific case of 20° to mimic a 3DCRT[32].

Dosimetric comparison for the different RT techniques has been reported in Appendix A, including analysis from phantom or in silico studies applied on previously irradiated patients.

Chapter 2

Breast Toxicity and QoL

Although the use of RT has been proved to be an effective adjuvant treatment for early-stage breast cancer patients, it is also true that ionizing radiation may cause damage to the parenchymal breast tissue, the skin, the lungs, the heart and the contralateral breast. The early lung toxicity (pneumonitis), cardiac events, and genetic mutations inducing secondary cancer in the contralateral breast (late complications) rarely happen, especially with the evolution of the RT machines. Moreover, a long observation time is needed for the late complications, with many years to manifest the event. Recent publications [34, 43] assessed 45% of acute radiological pneumonitis (changes in CT) and 11% of clinical pneumonitis with the need for corticosteroids. The mean onset time was 3 months after RT, and the most affected functional parameter was the total lung capacity. The symptoms are usually solved with time, but future studies to assess the impact of radiological pneumonitis on the development of radiation fibrosis and serial pulmonary function would be helpful, also for the dosimetric plan. Radiotherapy for breast cancer contributes little to the already high risk of second cancer in the opposite breast. Boice et al. reported that 3% of second breast cancers could be attributed to previous radiation treatment. The risk was significantly increased among women who underwent irradiation at a relatively young age ($\geq$45 years) as well as in patients with a higher average dose to the contralateral breast [13]. Okonogi et al. found a relative risk (RR) of contralateral breast cancer increased by 1.85-fold (95% confidence interval 1.05-3.26, median FU time 9.7 years) among patients compared with the general population. Burt et al. conducted an epidemiological study on 375000 subjects and contrary to many studies that have shown a statistically significant increase in contralateral BCs[56], they found that only approximately 0.8% of contralateral BCs were attributable to RT. In a recent cohort[90], Zhang et al. (2020) estimated the secondary cancer risks in organs after whole-breast irradiation using different radiotherapy techniques. The secondary cancer risks for tangential IMRT were slightly lower or similar to those for wedge 3DCRT but

considerably lower than those for multiple field-IMRT or VMAT.

Breast RT has been shown to be a risk factor for long-term increased heart failure, coronary artery disease, myocardial infarction and fatal cardiovascular events over 10 years after RT[25]. This limitation was more clear in the irradiation of left-sided breast cancers, where the mean cardiac dose can be several times higher than the right-sided[69]. Retrospective studies on the dose-response relationship between cardiotoxicity and the dose to the heart have highlighted a linear increase of cardiac events with the mean dose to the organ , defining quantitative constraints for RT planning. Recently, specific care for the lateral descending artery has been proposed on the optimization of treatment techniques in order to diminish the risk of later radiation-induced stenosis. Moreover, there is an increasing interest in the implementation of heart-sparing RT techniques in clinical practice[12, 64].

2.1 Skin Reactions

Concerning cosmetic alterations and skin reactions, they can occur more frequently and were investigated as a counterpart to evaluate the safety of new RT schedules. These events are side effects resulting from the accumulated damage to the epithelium during the RT fractions. Cells' rearrangement and the proliferation process lead to restoring the parenchymal tissue with skin esthetical and physical recovery. Even if the nature of acute side effects is transient in most cases, the partial radiation-induced changes can be painful and debilitating for the patient. Notably, the radiation-induced damage to the skin may also generate late complications that are often chronic and whose impact on patients' QoL is more deleterious than the early effects. There are at least three technical issues that have limited the availability of reliable results from investigations of the skin dose-response relationship for acute and late reactions: (i) the contouring of such organ is generally not foreseen in the breast RT protocol, (ii) the dose calculation from the TPS has unresolved uncertainties, (iii) it is unclear which part of the epidermis and inner layers should be responsible for the tissue reactions. To overcome all these aspects, studies in the literature often preferred investigating the relationship between radiation-induced skin alterations and the prescribed dose to the tumour as a surrogate of the involved tissues. Avanzo et al. quantified the difference between the measured superficial dose to the body and the TPS calculation through an in vivo dosimetric study using gafchromic films. The more the field entry is perpendicular to the tissue, the more significant the discrepancy between the measured and calculated dose [5]. The reduction can reach 30% of the prescribed dose according to the kind of treatment technique in the Head and Neck district[41]. Rudat et al. tested the differences in the breast district, showing

the 3DCRT superficial dose to be lower than with IMRT[66]. Almberg and colleagues performed a phantom study to derive an average dose level with depth to approximate the dose in the skin rescaling the prescribed dose to the target by a conversion factor[3]. They showed that the dose to 5 mm depth was 89.4% of the prescription dose for 3DCRT and 87.6% for IMRT. The Norwegian group also demonstrated that the difference is affected by the dose voxel size, with 2 mm representing the more realistic and robust computation in IMRT and VMAT[62]. It is reasonable to believe that radiation's early effect mainly affects the superficial and responsive part of the skin tissue, including the epidermis and the dermis. It is usually described as the first 5 mm layers[76]. Inflammation occurs within the first 24 h after the RT begins with the generation of free radicals and reactive oxygen in the rapidly dividing basal layer cells and dermis[55]. Radiotherapy damage accumulates through overtreatment, leading to delayed skin healing. A decrease in the stem cells, changes in endothelial cells and promotion of inflammation are among the biological consequences of radiation. During the weeks of treatment, sustained erythema develops, and it can manifest with local oedema and infiltration of leukocytes[14, 75]. Most of the time, the mild reactions are solved with the natural re-epithelialization that begins within ten days in standard conditions (can be prolonged with exposure to radiosensitizing drugs) without any symptoms or discomfort by the patient. Moderate acute toxicity, such as skin desquamation, dermatitis and painful edema, manifest by the end of RT, suggesting failure and complications in the keratinization process (usually completed in around 30 days). These events may significantly impact on patient's QoL but are generally transient and solved with topical agents within a few weeks after the treatment. Concerning limitation (iii), more uncertainties are on the pathophysiological process affecting late sequelae development. Indeed, chronic effects on the skin induced by radiotherapy are changes to the vasculature and connective tissue of the cutaneous and subcutaneous layers leading to telangiectasia, fibrosis, pain and hyperpigmentation of the skin. Available data suggest that chronic radiation dermatitis is caused by an imbalance of proinflammatory and profibrotic cytokines, which starts after irradiation and lasts for months or even years. These include tumour necrosis factor-alpha (TNF-alpha), interleukins 6 and 1 (IL-6 and IL-1), tumour growth factor-beta (TGF-beta), platelet-derived growth factor (PDGF), and connective tissue growth factor. TNF-alpha, IL-6, and IL- 1 are responsible for persistent inflammation, whereas TGF-beta and PDGF promote fibrosis by activating fibroblasts and inducing the synthesis of extracellular matrix proteins and matrix metalloproteinases[75]. The concomitant radiation-induced endothelium damage results in improper vascularization of irradiated skin and restricts blood perfusion. It may exacerbate fibrosis and deteriorate the healing process[40]. This phenomenon, together with the secretion of PDGF, can also play a role in the

pathogenesis of telangiectasia[29]. In addition, persistent inflammation and secretion of proinflammatory cytokines lead to leukocyte infiltration, which may cause other manifestations of chronic radiation dermatitis, such as skin atrophy or necrosis[15], which includes induration and retraction of the skin, lymph- oedema, joint motion restriction, changes in skin appearance, wounds, and ulcerations[28]. The fibrotic lesions are usually restricted only to the irradiated area, and adding a boost dose increases the risk of radiation-induced fibrosis[47]. For all these reasons, managing chronic effects is difficult because of the inability to differentiate injured tissue from uninjured tissue and the unpredictable inflammatory waves that can come weeks to years after tissue injury[75]. To conclude, it has to be mentioned that not in rare occasions, the acute radiation-induced damage fails to heal and evolves into consequential-late changes of RT, including chronic wounds and skin necrosis[29].

2.1.1 Grading and Timing for Skin Reactions

Several grading scales exist for reproducible assessment and documentation of radiodermatitis. The CTCAE (Common Terminology Criteria for Adverse Events) and the RTOG (Radiation Therapy Oncology Group) are the most common scoring system for skin toxicity.

CTCAE v4.0 has separate scales for radiation dermatitis (erythema) and skin ulceration (desquamation), which are relevant to the acute response to radiotherapy in the breast. Differently, RTOG is based chiefly on the target organ or body region (e.g., larynx, upper GI, skin). The typical time discrimination for acute and late effects is 3 months after RT. The time factor can be a problem primarily for late toxicity since the acute symptoms are usually scored at a single point at the end of the RT visit (sometimes trial registered even intra-RT time points for acute effects). For chronic symptoms, knowing the appearance time for the toxicity is extremely important to avoid partial and incorrect analysis of dosimetric and extra dosimetric risk factors. In any case, the longer the FU, the more accurate the analysis. For breast cancer, publications suggest 6 months for oedema [89]and 60 months for fibrosis[39]. This raised the issue of using different toxicity scales and assessment time points. Finally, to perform an analysis of the radiation-induced effects on cancer patients, a baseline measure before the start of RT is necessary to avoid wrong evaluation caused by patient history and comorbidities or by other neo-adjuvant treatments. More objective measures of radiation-induced skin toxicity have been suggested to overcome the inter-user uncertainty of subjective scales. Doppler fluxometry[68], hyperspectral imaging[1] and spectrophotometers[88, 21] are some of the tools introduced in the clinic to test the dose-response relationhsip and the association with questionnaire assessment.

2.2 NTCP models for skin toxicity

Predictive models for skin toxicity have been developed in the literature. Most of these models aim to incorporate the dose as a main predictive parameter describing the organ's dose-response relationship, i.e. a mathematical function that describes the tolerance of the tissue to radiation exposure. Usually, this relationship is a sigmoidal shape function and can be explained by different mathematical equations, with logistic regression considered the easiest to apply to the data. Such kinds of functions are suggested to fit binomial data (0,1). Consequently, if we use questionnaire scores as an independent variable, the previous grading scales have to be dichotomized according to the severity of the reaction we aim to describe. For instance, if we focus on the prediction of moderate-severe acute symptoms, we will consider grade 0 and grade 1 as our 0 (No Tox = patients who did not manifest moderate or severe symptoms), while grade 2, grade 3 and grade 4 will be defined as 1 (Tox patients group). In the case of quantitative data as the dependent variable, we have to apply a cutoff to transform a continuous variable into a binomial one. As a general rule, the steeper the function, the more the reaction is a threshold phenomenon, i.e., the effect of the response is deterministic over a specific dose value of the dosimetric descriptor. Planty descriptors can represent the dose variable. The most used are the single points of the DVH for at least two practical reasons: (i) they are simple to interpret and derive; (ii) they have the advantage of being directly applicable as dosimetric constraints to the TPS. Indeed, the final aim of a predicted and validated dose-response model is to identify a possible dose-volume constraint, i.e. a threshold value for that descriptor such that if the plan satisfies that condition, the patient has an acceptable risk of developing a specific side effect. With the evolution of radiobiological knowledge, models started to consider new parameters able to summarise the full information provided by the DVH. This is the case of the Equivalent Uniform Dose, which converts the real DVH into a homogeneous DVH (rectangular shape), receiving 100% of a new equivalent dose. It is expressed through the following law of power

$$EUD = \left(\sum_i \nu_i D_i^{1/n} \right)^n \tag{1}$$

with n representing the volume parameter, i.e., the organ's behaviour of being more compromised if large volumes receive a medium dose (parallel organ) or small volumes are irradiated with high doses (serial behaviour). Other options for dose descriptors are the dose surface maps, which, differently from DVH, include spatial information on the dose distribution and allow for the investigation of sensitive substructures within empty organs. For such organs, but also superficial structures like the epidermis, some applications considered the Dose Surface

Histogram (DSH), which is a DVH that takes into account only the dose delivered to the external surface of the organ. Regarding the dose information, it is essential to specify that in the case of multiple RT schedules, some mathematical precautions have to be taken to compare in an appropriate way dose distributions. Thus, exploiting the radiobiological LQ model is necessary to convert any dose into an EQD2 (equivalent dose to 2 Gy), and the radiobiological parameters of such conversion (the organ-specific alpha and beta, or more frequently α/β) have to be fitted or derived by clinical or preclinical studies. Moreover, such dosimetric models can be enriched by including other significant factors (treatment characteristics, patient information, genetic features) representing a risk for toxicity development. It is worth noting that with the current advances in RT techniques, the role of the dose is no more the predominant, with some side effects manifesting a multifactorial nature in their dysfunctional process. In other words, individual biological features create differences between the patient and population response curves, making some subjects more radiosensitive than others. The studies presented in sections 2.3.1 and 2.3.2 are retrieved from Chapter 12, "Adverse Effects to the Skin", written by M. Avanzo, J Stancanello and R. Jena and included in the book "Modelling Radiation Side Effects"[63].

2.2.1 Predictive models for acute symptoms

Most of the reported models were developed in the era of the orthovoltage (200kV) photon beams RT. LQ model was considered to correct the dose in different fractionation schemes, while relative biological effectiveness was applied to evaluate the equivalence in the contribution of the electron beam (12-13 MeV) with respect to 200kV photons. The study by Turesson and colleagues assessed the erythema and the moist desquamation by the use of a spectrophotometer, registering toxic changes of more than 50% (compared to the baseline value) in the characteristic wavelength for oxyhemoglobin (578nm) and melanin ($>$ 660 nm)[80]. The α/β ratio for these endpoints was fitted, resulting in α/β of 7.5 Gy and 11.2 Gy, respectively. Pastore and colleagues analyzed the severe acute toxicity based on the RTOG score of 140 patients treated with 50 Gy + 10 Gy of electron boost[59]. The dosimetric descriptor was the DSH at 3mm from the patient body contour with a cut to the histogram below 5 Gy as non-representative of the breast region. The absolute DSH was then normalized based on this volume cutoff. They found S30 Gy associated with severe acute toxicity. The n value for the superficial organ was 0.4.

2.2.2 Predictive models for chronic reactions

The most studied late symptoms were telangiectasia and fibrosis. Turesson and Bentzen studied the former. The α/β ratios of 2.8 and 3.7 Gy (including complete repair correction) were identified. For fibrosis, an α/β of 1.9 Gy was proposed by Bentzen[11]. Alexander et al. reported a parallel behaviour of the skin for fibrosis development (n=0.78)[2]. Avanzo and Mukesh[6, 53], after LQ correction with $\alpha/\beta = 3Gy$, found volume parameters n of 0.15 and 0.012, respectively, suggesting a a highly serial behaviour of the skin when large datasets are analyzed. Moreover, the results from the Mukesh group were also validated on an external dataset from the START-pilot trial. An intermediate volume parameter was found by Emami et al. to describe necrosis and ulceration. In this study, the irradiated area was normalized to $100cm^2$.

References	End-Point	Dataset	Model, Parameters	Notes	EQD2Gy5%, EQD2Gy50%
			A		
Turesson and Thames (1989)	Erythema	Breast orthovoltage RT	LQ model ln(K) = 4.81, α = 0.95•10^{-1}, β = 1.27•10^{-2}, α/β = 7.5 Gy	No surface effect, electrons RBE = 0.83	30.8 Gy, 43.8 Gy
Turesson and Thames (1989)	Moist Desquamation		LQ model, ln(K)=5.57, α=1.02•10^{-1}, β =0.91•10^{-2}, α/β = 11.2 Gy		37.2 Gy, 49.4 Gy
Present study	Grade ≥2 Dermatitis	Published studies on breast RT with MV-photons, Table 12.2	Lyman, D_{50} = 58.3 Gy, m = 0.28, α/β = 10 Gy	Assumed skin dose 90% of prescribed. Electrons RBE = 0.89	29.5 Gy, 58.3 Gy
Present study	Moist Desquamation		Lyman, D_{50} = 55.8 Gy, m = 0.22, α/β = 10 Gy		33.1 Gy, 55.8 Gy
Burman et al. (1991)	Ulceration/Necrosis	Based on previous model by Von Essen (1973)	Lyman, n = 0.1, m = 0.12, D50 = 70 Gy	Reference surface 100 cm^2, no correction for fractionation	55 Gy, 70 Gy
Pastore et al. (2016)	grade ≥3 RTOG Toxicity	Single institution breast cancer dataset	Lyman, n = 0.38, m = 0.14, D_{50} = 39 Gy	No correction for ractionation	30.2, 39 Gy
			B		
Turesson and Thames (1989)	grade ≥1 Telangiectasia at 3 years	Breast, orthovoltage	LQ model ln(K)=3.98, α=0.48•10^{-1}, β=1.73•10^{-2}; α/β=2.77 Gy	No surface effect considered, RBE = 0.83 for electrons	34.9 Gy, 52.6 Gy
Turesson and Thames (1989)	grade ≥2 Telangiectasia at 5 years	Breast, orthovoltage	LQ model ln(K)=5.36, α=0.64•10^{-1}, β = 2.29•10^{-2}; α/β=2.79 Gy		38.8 Gy, 52.2 Gy
Bentzen and Overgaard (1991)	Telangiectasia	Post mastectomy	Logit function and LQ Model with complete repair, α0 = −8.6 α= 0.099 Gy −2, β= 0.036		33.1 Gy, 50.3 Gy
Present study	Telangiectasia	Published studies on breast MV-RT, Table 12.2	Lyman, D_{50} = 58.2 Gy, Lyman, m = 0.11, α/β = 3 Gy	Assumed skin dose 90% of prescribed, Electrons RBE = 0.89	47.4 Gy, 58.2 Gy
Avanzo et al. (2012)	Subcutaneous Fibrosis	Published data	Lyman, D_{50} = 107.2 Gy, m = 0.22, n = 0.06, α/β = 3 Gy		47.3 Gy, 73.7 Gy
Mukesh et al. (2013b)	Subcutaneous Fibrosis	Data from 3 trials	Lyman, D_{50} = 132 Gy, m = 0.35, n = 0.012, α/β = 3 Gy		34.5 Gy, 81.4 Gy

LQ=linear quadratic; MV=megavoltage; RBE=Relative Biological Effectiveness.

Figure 3: Summary of the existing model for (a) acute and (b) late toxicity to the skin. Table extracted from [63]

However, these studies were performed on patients treated with orthovoltage radiation and post-mastectomy, and any attempt to extend them to the current clinical practice can be unsafe. Even if we neglect the possible impact of the mastectomy (compared to the most currently spread lumpectomy) on radiation-induced skin alteration, there are still too many uncertainties about the RBE of

Authors	Technique	PTV Dose/Fractions	Boost Dose/ Fractions/% of Patients	Total EQD2Gy	Patients	End-Point
Keller et al. (2012)	Hybrid IMRT	46 Gy/23 fx	14 Gy/7 fx/99%	60. 1 Gy	946	Telangectasia 8.2%
Haviland et al. (2013) START-A	3D-CRT	50 Gy/25 fx, 41.6 Gy/13 fx, 39 Gy/13 fx	10 Gy/5 fx/60%	56.9, 55.0, 53.8 Gy	730, 730, 627	Telangectasia 5.7/5.9/2.5% at 10 years
Haviland et al. (2013); START-B	3D-CRT	50 Gy/25 fx, 40.05 Gy/15 fx	10 Gy/5 fx/60%	56,9/52.4 Gy Gy	1081/1094	Telangectasia 4.8/3.1% at 10 years
Lilla et al. (2007)	3D-CRT	50.4–50 Gy/25–28 fx	12 Gy/6 fx/90%	59.5 Gy	409	Telangectasia 31.8%
Jagsi et al. (2015)	3D-CRT	50 Gy/25, 40.05 Gy/16 fx	10 Gy/5 fx, 93%/60%	54.1/43.5 Gy	1731/578	MD 28/6.6%
Pignol (2008)	IMRT, 3D	50 Gy/25 fx	16 Gy/8 fx/30%	54.8 Gy	170/161	MD 31.2/47.8%
Chen et al (2010)	3D-CRT	50.4 Gy/28 fx		49.56 Gy	158	MD 23%
De Langhe et al. (2014)	IMRT	50 Gy/25 fx, 40.05/15 fx	10 Gy/4 fx/75%	57.8, 50.1 Gy	45/332	MD 51.1, 9.9%
Rudat et al. (2016)	Inverse IMRT/3D-CRT	40.05/15 fx, 50 Gy/25 fx	Evaluated before boost	42.3 Gy, 50, Gy	121/145	AD2 2/19%
De Langhe et al. (2014)	IMRT	50 Gy/25 fx, 40.05/15 fx	10 Gy/4 fx/75% patients	57.8, 50.1 Gy	45/332	AD2 87, 54.5%
Nagai et al. (2017)	IMRT Tomodirect	50 Gy/25 fx		50 Gy	152	AD2 ≥ 2: 15.8%
Freedman et al. (2009)	3D-CRT/IMRT	48 Gy/24 fx	14–20 Gy/95% patients	63.2 Gy	60/73	AD2 75/52%
Harsolia et al. (2007)	IMRT/3D-CRT	45 Gy/25 fx	16 Gy/8 fx	52.7 Gy	93/79	AD2 41/85%
Jagsi et al. (2015)	3D-CRT	50 Gy/25, 40.05 Gy/16 fx	10 Gy/5 fx, 93%/60% patients	54.1/43.5 Gy	1731/578	AD2 61/27%
Monten et al. (2017)	VMAT	28.5 Gy/5 fx, 33.5 Gy/5 fx		32.3 Gy/40.3 Gy	32/63	AD2 0/17.5%
Hijal et al. (2010)	3D-CRT	42.6 Gy/16 fx		39.6 Gy	162	AD2 11.7%

PTV=Planning Target Volume; IMRT=Intensity Modulated Radiation Therapy; 3D-CRT=three-dimensional Conformal Radiotherapy; VMAT=Volumetric Modulated Arc Therapy; fx=fractions; EQD2Gy=2Gy equivalent dose; MD=moist desquamation; AD2=grade ≥ 2 acute dermatitis.

Figure 4: Summary of studies reporting toxicities to the skin used to derive dose response in the meta-analysis from Avanzo and colleagues. Table extracted from [63]

photons when moving from orthovoltage to megavoltage treatments. In the Chapter "Adverse Effects to the Skin", the authors presented a meta-analysis of the most recent studies (listed in Figure3), considering (i) the skin maximal dose is 90% of the prescription dose to the PTV, (ii) an RBE for electrons of 0.89[11], (iii) doses converted in EQD2 with α/β 10 Gy for acute symptoms and 3 Gy for late effects, (iv) the number of patients in the cohort used as a weight in the meta-analysis coefficient determination. The endpoints were acute grade$>$ 2 dermatitis [ranging from 0 – 85%] and most desquamation [9.9 – 51.1 %], and late grade$>$ 2 telangiectasia [3.1 – 8.2%]. Three dose-response relationships were established, demonstrating increased toxicity for raising the prescription dose; fitting parameters for the models are included in Figure 4. Lazzari et al. analyzed the Ontario trial (42.56 in 16 fr without a boost of RT) and identified, among the available parameters, the PTV volume and the hotspot (V110%) as associated with grade 3 late toxicity[48]. Also, Ciammella et al. found a relationship between PTV hotspots and late subcutaneous toxicity[20]. No association between hotspots and cutaneous (acute and late toxicity) was identified. A novel approach was presented in the analysis by Alexander and colleagues[2]. They remarked that using prescribed doses rather than dose distributions from the clinical studies implies a

loss of information about the original treatment. As already discussed in Chapter 1, the assumption is that different techniques produce different homogeneity in the dose distribution, which must be considered. The authors performed a phantom study to assess differences and reduce the PTV DVH shape to treatment parameters. Following this method, it is possible to derive a synthetic DVH for every group of patients treated with similar treatment characteristics. Then, they applied the results to a meta-analysis for late fibrosis based on the EUD and BED from the synthetic PTV DVHs. Recently, Kindts and colleagues developed an NTCP model for late unfavourable aesthetic outcomes using the EUD derived from the breast DVH[44]. The volume was delineated according to the EORTC guidelines but included the 5 mm of the breast skin (PTV+skin). In addition, plans during the recruiting time were developed using two different software (Pencil Beam, AAA). The study analyzed patients treated with conventional or Canadian schemes followed by an RT boost. Doses were previously converted to EQD2 with $\alpha/\beta = 3.6Gy$, as identified by Bentzen[11]. Mean EQD2 dose (OR 1.18) and several DVH points (V30 Gy to V45 Gy + V55-V65 Gy with OR from 1.42 (V35 Gy) to 1.09 (V65 Gy)) were reported as risk factors. To summarize, the presented studies showed efforts to exploit the information from several past trials retrospectively. The most straightforward method was to consider the prescription dose to the PTV and derive macroscopical insights from the incidences in the several schemes of RT. The assumptions were (i) the seriality of the tissue involved in the skin reactions, (ii) a proportionality with the maximal dose to the skin, and (iii) a description of the average dose to the subcutaneous and fatty tissue. When Aamberg verified point (ii), the evolution was to consider a surrogate of the maximal dose to the skin according to the treatment characteristic. Nevertheless, the seriality of the dermis has not been extensively proved. Consequently, the information coming from the DVH could be necessary to classify the patients at risk of reactions correctly. To do this, the surrogate PTV plan DVH[2] could help improve the discrimination in populations treated with similar schemes but different techniques. Such an approach does not consider the variation in the homogeneity due to the breast size. In this sense, the PTV + skin DVH by Kindts represents the most accurate dosimetric set to investigate skin reactions, even if non-responsible tissue could be considered, creating noise, especially for acute symptoms. A proper rigorous way to perform a dosimetric analysis of such endpoints could be: 1) to consider together the metric from the skin (tissue from the external body to 5 mm in depth) and PTV, without any overlap between the two; 2) to define different subcutaneous regions (concentric) from the skin toward the thorax and compute subanalysis for each endpoint, defining which is the more appropriate to describe that specific toxicity.

Table 2: Literature findings for breast volume in acute and late skin reactions.

Paper	Parameter	Threshold	Endpoint	OR	pts
Moody et al[51]	Breast Volume	Small-medium-large (by photograph)	Late radiation changes		559
Lazzari et al[48]	Breast Volume	PTV<1300cc	Late toxicity / Cosmesis	9.6	215
Back et al[7]	Breast Size	19 cm	Moist desquamation G2+	3.6	234
Barnett et al	Breast Volume	Continuous	Telangiectasia	3.94 per L	1014
			Oedema	3.65 per L	1014
			Pigmentation	1.75 per L	1014
			Pain	1.29 per L	1014
Kraus-Tiefenbacher et al[45]	Breast Volume	Continuous	Acute Skin toxicity	1.001	211
Back et al[7]	Weight	>70 Kg	Moist Desquamation G2+	2.1	234
Barnett et al[8]	Weight	Continuous	Telangiectasia/ Oedema	1.04	1014
Pignol et al[61]	BMI	Continuous	Moist Desquamation	1.16	358
Kindts et al[44]	BMI	Continuous	Edemea	1.09	121
Pignol et al[61]	Breast cup	A vs B-C, A vs D	Moist Desquamation	3.6	358
Pezner et al[60]	Breast cup	A-B vs Other	Oedema	15% vs 48%	47
Clarke et al[35]	Breast cup	A-B vs C-D	Cosmesis	3% vs 17%	
Raw et al	Breast cup	A-B vs C-D	Cosmetic	8% vs36%	130
Brierley et al[16]	Breast Cup	A-B vs C-D	Fibrosis	9% vs 36%	133

2.2.3 Other factors influencing the skin reactions

Breast volume One of the most common identified risk factors is breast volume or any correlated factor (breast cup size, Body mass index, Obesity, Breast Diameter). There are two possible explanations for this recurrent result. The first is explained through the functional subunits (FSUs) and the concept of the functional reservoir[86]. According to this theory, a certain number of FSU in the skin (Archambeau and colleagues have investigated and defined the structure of a skin FSU[4]) has to be compromised to lead to symptomatology. The basal layer can contribute to attenuating the damage in the epidermis through the production of basal cells that go to restore the cells' death in the FSU. For a structural reason, the basal layer is thinner than the epidermis; thus, for larger breast volumes, we have a more considerable disproportion between the damaged tissue and the "cell bank". Another explanation is dosimetric. Indeed, women with large breasts may receive a more inhomogeneous dose distribution with a higher probability of local hot spots[51, 54]. Some studies [87] investigated the superficial extension of such hot spot regions using DSH, and some others considered points in the tail of PTV DVH[27, 20], identifying relationships with both acute and chronic symptoms. As already discussed, this method does not allow considering the contiguity of such a hot spot, which seems to be a critical condition according to the presented reasons. In the orthovoltage application, studies highlighted that the maximally tolerated dose depends on the irradiated area through a negative power law. From a practical point of view, categorizations were created to determine patients at risk. Michalski proposed three classes of volume with the following thresholds: large volume $\geq 1.600cm^3$, intermediate $975 - 1.600cm^3$, and small $\leq 975cm^3$. A table of the results concerning the volume relationship with the skin endpoints is reported in Figure5.

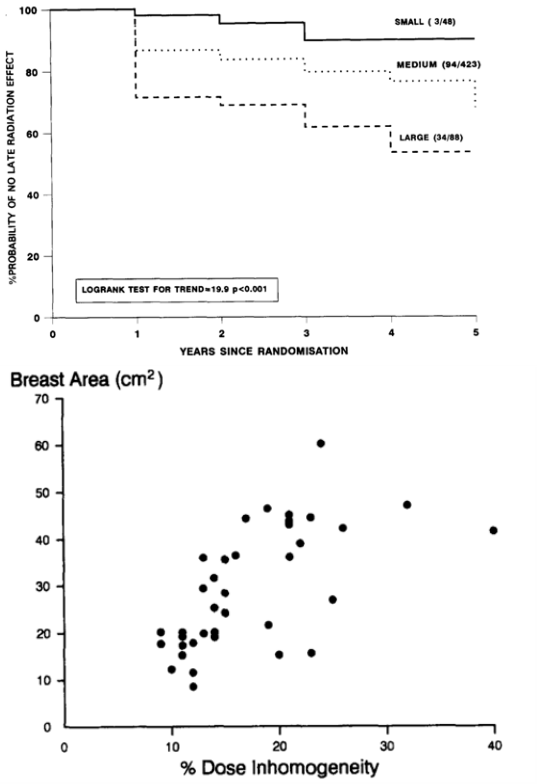

Figure 5: a) Breast Volume impact on late radiation effects (extracted from [51]; b) Relationship between the Breast Area and the Dose Inhomogeneity (extracted from [54].

Other Factors Several clinical and treatment factors have been investigated with primary dosimetric descriptors, with the analysis of Barnett as the most extensive in the field[8]. Table3 reports a list of the features retrieved by these papers. Diabetes mellitus is frequently hypothesized to be a risk factor for increased late toxicity from radiotherapy in various tumour sites. Indeed, chronic diabetes can cause occlusive microvascular changes and increased blood viscosity generating tissue hypoxia and decreasing the ability to perfuse and heal irradiated normal tissue.Late toxicity has also been shown to be more relevant in smokers after radiotherapy to the head and neck, and it has been postulated that the vascular-toxic effects of smoking and radiation combine to increase the severity of late tissue injury. Nevertheless, in breast toxicity, current smokers have shown to develop more acute symptoms, suggesting that smoke can alter mainly the microvasculature in the peripherical part of the body, such as the skin. Associations have been found between chemotherapy and skin toxicity, especially concurrent chemo-radiotherapy. In breast cancer, it has been identified as a risk factor for

skin symptoms and cosmesis [7, 23, 20, 44]. Back et al. reported that concurrent chemotherapy was worst than sequential with 42% vs 27% for most desquamation in the two groups [7]. Moreover, Eleven patients required an unscheduled break in the delivery of their radiation therapy, owing to either cutaneous or haematological toxicity. Nine of these 11 patients were treated with concurrent chemoradiotherapy. The study by Barnett found a protective role of the CHRT. They argued it could be obtained by chance (the study population was $ge1000$ patients), or it could be a surrogate of the time delay between surgery and RT, giving complicated surgeries the time to wound healing before the RT start. On the same line, the breast resection volume in surgery was identified as a risk factor for acute toxicity and oedema, suggesting that larger surgical volumes could need more time to regenerate, and RT treatment should be scheduled considering this information. Tamoxifen treatment was associated with both acute and late symptoms. However, its relationship with age and menopausal status have to be considered, while aromatase inhibitors were associated only with acute moderate toxicity. Age (protective factor for pain), allergies and axillary lymphadenectomy were found as risk factors in the listed studies in Table3. There were also studies reporting the T stage as a complication factor, but there is no explanation to believe that this result was not only obtained by chance. Moreover, several studies have reported the RT boost (yes vs no yes [20, 23, 27] as a risk factor in skin reactions. Few of them found the importance of the boost volume or the radiation source. For instance, the 10-year follow-up from the large EORTC study showed that the administration of a 16 Gy radiotherapy boost improves local control but approximately doubles the risk of fibrosis [40]. In general, boost information should be addressed through DVHs and RBE conversion, but some limitations make this process hard to perform, especially if the boost is sequential and Is delivered with a non-photon source. An aspect to mention is the importance of acute response[23] as a predictor of the development of chronic symptoms. A consequential effect is typically defined as a late effect that has been caused by a particularly severe acute reaction[31, 11]. The relationship between early and late effects of radiotherapy is unlikely to be strong after adjusting for dose fractionation and patient-related factors. As the last aspect to consider, it has been estimated that around 70% of individual variation in late normal tissue toxicity may be due to genetic factors in studies where the radiotherapy dose-fractionation schedule was identical[18].

Table 3: Example from literature of other factors influencing acute and late skin reactions.

Paper	Factors	Endpoint	OR	pts
Barnett et al[8]	Diabetes	Breast Oedema / Shrinkage	1.64/ 2.08	1014
Ciammella et al[20]	Diabetes	Late Subcutaneous Toxicity	n.r.	212
Barnett et al [8]	Smokers	Pigmentation	2.06	1014
Kraus-Tiefenbacher et al[45]	Smokers	Erythema G2	n.r.	211
Barnett et al [8]	Chemo	Acute toxicity	0.62	1014
Ciammella et al [20]	Chemo	Late subcutaneous Toxicity	2.6	212
Back et al [7]	Chemo	Most Desquamation	n.r.	223
Collette et al [23]	Chemo	Fibrosis	2.40 / 2.55	2606/2572
Kindts et al [44]	Chemo	Late cosmesis	2.56	121
Collette et al	Tamoxifene	Fibrosis	1.55	2606
Barnett et al [7]	Tamoxifene	Acute Skin Toxicity	1.23	1014
Kraus-Tiefenbacher et al[45]	Tamoxifene	Acute Skin Toxicity G1	n.r.	211
Kraus-Tiefenbacher et al [45]	Aromatase inhibitors	Acute Skin Toxicity G2	n.r.	211
Bernett et al [8]	Age	Telangectasia/Oedema/Pain	1.32/1.84/0.81	1014
Kindts et al [44]	Axillary lymphadenectomy	Late Cosmesis	3.17	121
Kindts et al [44]	Surgical Specimen weight (g)	Late Cosmesis	1.02	121
Back et al [7]	Breast Volume resected	Acute Skin Toxicity	n.r.	223
Kraus-Tiefenbacher et al[45]	Allergies	Acute Skin Toxicity G2	n.r.	211

Chapter 3

Materials and Methods

3.1 Thesis Objectives

Here, we present a study on acute and late skin reactions in early-stage breast cancer patients treated with adjuvant radiotherapy. The study population is a large cohort of patients treated in a single institute with the same radiotherapy schedule. The analysis investigated clinical and dosimetric factors with the primary aim of obtaining a dose-response relationship for the breast skin for the first time. The advantages of such a study are the presence of CT skin delineation (5 mm layers), the univocal institutional treatment recommendation, the long follow-up time, the homogeneous RT scheme and the statistical power to investigate moderate reactions reducing the intrinsic bias that is present in the evaluation of mild effects.

3.2 Study Population

The study population consists of 1325 consecutive BCa patients who underwent conservative surgery for a pTis-pT3 pNxpN1a M0 disease and were treated with RT at San Raffaele Hospital between February 2009 and May 2017. The radiation treatment was a whole breast hypofractionated scheme delivering 40 Gy in 15 fractions without boost independently of age, obesity, breast volume, side, chemotherapy/trastuzumab prescription, and comorbidities. Patients in the study were treated with a Varian DHX and 6-100 Linacs. All patients signed informed consent for treatment and permission for publication of disease-related information following the Helsinki Declaration. The institutional ethics committee approved the retrospective revision of patient outcomes and a prospective study of the quality of life of BCa patients treated with hypofractionation, registered to ClinicalTrials.gov (NCT03077191: Toxicity and Outcome of Whole Breast Hypofractionated

Radiotherapy: a Single Institution Experience). Patients were treated supine on a posiboard, with arms above the head. CTV was defined as the whole breast on CT scan images acquired with a 5 mm step, consistently with national guidelines. Planning target volume (PTV) was generated by the expansion of CTV with 5-10 mm margin in all directions except the lung (5 mm); a crop to the body was made to eliminate the first 5mm of skin. None of the patients had a regional lymph node (LN) irradiation prescription. The heart, lungs and contralateral breast were delineated, and the body was automatically generated. A median number of 4 segments was used (ranging from 2-11) within a tangential 3DCRT technique to obtain homogeneous dose distribution within PTV, with hotspots $\leq$ 108% on PTV, covered by at least 95% isodose, and with 3% of the heart $\leq$ 40 Gy, and $\leq$ 20% of ipsilateral lung $\leq$ 17 Gy. Dual energies (6 MV, in the majority, and 18 MV) with different weighting factors and wedges were used as needed. Due to the complexity and the number of fields, the technique may be considered as a forward optimized IMRT and called as F-IMRT. The clinical practice for treating early breast cancer with adjuvant RT was stable over the years. The only variation was the use of bolus. In the first years, a 0.5-1 cm water-equivalent plastic bolus was admitted to improve PTV coverage in the regions next to the skin (used in 313 patients), mainly for 5 to 7 fractions. It was abandoned after an unpublished analysis observed an increase in toxicity. Daily patient positioning was corrected through CBCT. Patient and treatment characteristics are summarized in Table 4 5.

3.3 Follow-Up and Toxicity Scoring

Patients were visited twice during the treatment, reporting acute toxicity according to the RTOG scale[33]. Follow-up visits were scheduled at 6-18-30-42-54-66 months. The scheduling of follow-up visits was based on the report of Beadle et al, of the evolution over time of skin toxicity in breast cancer patients treated with breast conservative treatments and postoperative radiotherapy with standard fractionation[10]. The intent was to intercept late toxicity and intervene in patients where necessary with the available local/ systemic therapies. The SOMA-LENT toxicity scale was used to assess late collateral effects by combining physician examination with patient self-reports, increasing reporting accuracy. Two aesthetic results, one after surgery and one after RT, were scored by two observers through patient-reported, clinically and with photographs (taking the worst rating of these three evaluations). Radiation oncologists were encharged during the years to enrol patients and fill in the dataset with toxicity scores, patient characteristics, clinical features, and treatment factors, including selected dosimetric data.

Table 4: Patient and treatment characteristics of the study cohort.

Total nr. of patients	1325
Age groups (years)	
<45	133 (10%)
45-55	312 (23.5%)
55-65	322 (24.3%)
>65	558 (42.1%)
Age at diagnosis (median [IQR])	62.0 [51.1-70.5]
Side	
Right	640 (48.3%)
Left	685 (51.7%)
Chemotherapy	
No	954 (72%)
Yes	371 (28%)
Chemotherapy Type (371 patients)	
Anthracycline	295 (79.5%)
Taxane based	53 (14.3%)
Other (CMF, Capecitabine, etc.)	23 (6.2%)
Trastuzumab	
No	1216 (91.8%)
Yes	109 (8.2%)
Hormonal Therapy	
No	261 (19.7%)
Yes	1064 (80.3%)
Breast size	
Small	232 (17.5%)
Medium	423 (31.9%)
Big	459 (34.6%)
Very Big	211 (15.9%)
Obesity	
No	968 (73.1%)
Yes	315 (23.8%)
NA	42 (3.1%)
Diabetes	
No	1129 (85.2%)
Yes	78 (5.9%)
NA	118 (8.9%)
Smoke	
Smokers and former smokers	263 (19.8%)
Non smokers	1062 (80.2%)
Alcohol consumption (declared)	
No	1267 (95.6%)
Yes	58 (4.4%)
Hypertension	
No	761 (57.43%)
Yes	451 (34.04%)
NA	113 (8.53%)
Thyroid illnesses	
No	1025 (77.36%)
Yes	181 (13.66%)
NA	119 (8.98%)

Table 5: RT treatment characteristics of the study cohort.

Treatment type	
3DCRT	100%
IMRT	0%
Photon Energy Beam	
6MV	100%
¿6MV	0%
Number of segments	
2	29%
3	4%
4	59%
5-6	4%
8-9-10	4%
Bolus application	
No	78%
4-5 fractions	7%
6-7 fractions	7%
8 fractions	3.8%
9+ fractions	3.2%
Dose Boost	
No	100%
Yes	0%

3.4 "Skin" structure Delineation

Aiming to explore the possible causality between the damage to the cutaneous tissue and the acute and late reactions, we focused on the dose distribution of the skin, defined as the first 5 mm body layers (see Figure 6). We selected such thickness to follow the tissue alteration measured in the epidermis, dermis and hypodermis by Liu and colleagues through ultrasonic images after breast RT [50].

As already mentioned, this structure is not routinely contoured in the conventional breast RT protocol. To overcome this limitation, we built an automatic workflow in MiM Software that was able to automatically export the DVH for the aforementioned structure in 4 steps:

- read the input file; import from a path folder the DICOM RT file, including CT scan, RT struct and RT Dose files;
- structure delineation; it generates a 5 mm crop of the external body delineation (5mm_BODY), then a new structure "Skin" is defined as the Boolean intersection between the external body and 5mm_BODY;
- total dose computation; if the plan consists of more than one course of treatment (see patients treated with bolus), the software provides the dose distribution for the sum plan;

- dvh extraction; the absolute cumulative DVH for the "Skin" is exported as a csv file with dose steps of 0.1 Gy.

After retrieving all the available DICOM RT files and putting them in the specific path folder, the software extracted the DVH files all at once. It is worth mentioning that we performed a preliminary analysis to evaluate the PROs and CONs of a more accurate structure defined by taking into account only the intersection between the previous "Skin" and a PTV expansion of 0.5 cm in the axial direction and 1 cm in the lateral and cranio-caudal dimension [83, 67, 26]. The DVHs were equivalent for doses larger than 5 Gy; therefore, for practical reasons is more comfortable to use the previously described system in the daily clinic and apply a cutoff to histogram contribution < 5 Gy (it can help if you plan to apply relative constraints or EUD based constraints). This option is also supported by the findings of the section on the calculation algorithms. Moreover, the grid size for the dose was 2 mm3, in line with recomentation in the literature for skin dosimetry studies based on dose calculation algorithms[62].

3.5 Study Endpoint, observational time and investigated variables

A previous study was published on this population, investigating the time scale of skin response[33]. Given the low probability of development of late toxicity in a group of patients treated with a homogeneous dose distribution without boost, based on a previous report of the late skin toxicity evolution timescale in patients treated with standard fractionation[10] and on the pathophysiology of different late toxicities registered[14], the authors decided to create two toxicity groups for the analysis of the temporal evolution of late skin toxicity in patients treated with moderate hypofractionation: edema-hyperpigmentation (EH) and fibrosis-atrophy-telangiectasia-pain (FATP). We decided to preserve this toxicity grouping and also include an analysis of liponecrosis as specific additional injury of the breast tissue. Since the patient had different FU times, we applied a time threshold for each analysis based on the previous consideration of Fodor and colleagues. Specifically, EH toxicity was present mainly at six months after RT and decreased with FU time, while for FATP they identified an increasing incidence with time, with 42 months as the best period for toxicity analysis. Liponecrosi was not an endpoint of that study, but due to its late appearence, we applied the same time threshold as in the case of FATP (see Table 6 for a summary). Moreover, due to the large population size, we preferred to analyze a moderate-severe grade for both the toxicity endpoints; thus, patients with G0-G1 were labelled as 0, while G2-G3 was reported as 1. This choice will reduce the statistical power of the results but

Table 6: Summary of the Endpoints studied in the Thesis.

Endpoint	**Acronymous**	**Timing (within)**	**Grade**
Any Acute Toxicity	ACUG2+	End of RT	G2-G3
Oedema and Hyperpigmentation	EH	6 months after RT completion	G2-G3
Late Fibrosis-Atrophy-Telangectasia-Pain	FATP	42 months after RT end	G2-G3
Liponecrosis		42 months after RT end	Event

will improve the potential role of the dose or at least limit the importance of factors possibly contributing to the development of mild symptoms. The following available variables were considered: treatment duration, the time between surgery and RT, axillary lymph node dissection (ALND), in situ histology, vascular invasion, chemotherapy, monoclonal antibody, hormonal therapy, number of RT segments, bolus (yes/no), bolus fractions, PTV volume, PTV V105%, PTV V95%, Body D1%, cosmetic features at baseline, age, obesity, diabetes, hypertension, thyroid disorders, tobacco consumption (smokers and former smokers vs non-smokers), alcohol consumption and the "Skin" dosimetric variables. Specifically, points of dose from DVH were analyzed at decreasing steps to reduce the variable collinearity and define easy-to-apply constraints. The decreasing steps followed the irregularity of the average DVH, i.e., a steep fall at the very first Gy, a plateau from 10 Gy to 30-35 Gy and a final decrease toward the prescription dose. The investigated DVH points were V10 - V15 – V20 – V 25 – V30 – V34 – V36 – V38 – V40 – V41 – V41.5 – V42 – V42.5 – V43 Gy.

3.6 Statistical Analysis

Average DVHs for patients with and without toxicity were computed for each described endpoint. T-test statistics were applied to the DVH points in the two groups. The association of dosimetric and clinical factors with the endpoint was tested through univariate analysis. Significant factors to the univariate analysis (p-value< 0.10) were tested in multivariate models. The analysis was performed on the entire population, and the subgroup of patients treated without bolus. The reasons are the increased toxicity in that group and a more practical application of the dose constraints for the standard population due to the unusual application of the bolus in current breast RT practice. Moreover, to overcome the limitation of the lack of a baseline toxicity questionnaire, we performed a sub-analysis considering the cosmesis after surgery as an indicator of the impaired baseline condition. Finally, we computed sigmoidal dose-response curves through logistic regressions. The model perfromance was evaluated thorugh calibration plots, discrimination was assessed by the Area under the ROC curve (AUC) and goodness of fit thorugh Hosmer-Lemeshow test. Dosimetric constraints for the identified

DVH points were retrieved by the NTCP curves, considering, when applicable, acceptable toxicity risk below 5% and 10%.

3.7 Uncertainties due to the use of different dose calculation algorithms

Patients of the investigated cohort were treated over a considerable period of time; due to this, system upgrades occurred with changes in dose calculation algorithms implemented in the Eclipse TPS. Two main changes have been reported from using the Pencil Beam convolution (PBC), excluding the software update within the same algorithm. The first introduction was the analytical anisotropic algorithm (AAA) beam model for dose calculation; then, in 2015, the Acuros XB (AXB) algorithm was installed. Except in a few cases, the RT breast treatment moved directly from the PBC to the AXB. Further details on the characteristics of such algorithms are reported Appendix B. The different performances of the two algorithms (PBC and AXB) have been largely investigated in the literature for topical districts and organs but in a pretty limited way for the skin tissue in the breast. Nevertheless, predicting skin dose by commercial TPS is critical, as skin dose toxicity significantly impacts how well a patient tolerates the treatment. It is known that model-based dose calculation algorithms have limitations in the superficial regions (build-up regions), where the charged particle equilibrium (CPE) is not established, and the dose distribution within superficial depth mainly comes from contaminant electrons and secondary electrons. In addition, the performances critically depend on the quality of the implementation of the algorithms and can then vary between Institutes even using the same algorithms. Panettieri et al. [57] and Cao et al.[19], in two phantom studies, have shown that: (i) AXB, MC, and Gafchromic films have a good agreement, (ii) skin dose errors vary with the entrance angle, and the tangential field, the discrepancy with MC were 1.5% (AXB), 18.2% (AAA) and 3.3% (PBC), (iii) the grid size strongly affects the PBC build-up computation (need of a 2.5mm matrix) while it does not influence the AAA, (iv) in the first millimetre of depth the PBC tends to overestimate the dose for smaller angles and underestimate it for the larger angle of incidence, while the AAA overestimates absorbed doses against MC results for all angles of incidence and at all depths. This AAA behaviour seems to be due to the electron contamination model, which is not entirely able to provide perfect calculations in the build-up region. Finally, it has been found that for the space surrounding the body of the patient, the TPS forces the isodose lines to be closed inside the body contour of the patient while the MC estimates the dose in every voxel even in the surrounding air taking into account correctly the scattering component of the patient. For these reasons,

we performed an in-silico analysis on the impact of the three algorithms on the 5mm skin DVH in our real-life scenario. We selected a group of patients without bolus: three treatment plans were computed with different algorithms. Beam parameters were maintained as in the approved plan, and the only condition we imposed for a correct comparison was that the delivered MU were the same for all the plans with a tolerance of +-5 MU for multiple segment treatments. Average DVHs were computed, and a t-test was applied to DVH points to compare the differences in the dose distribution.

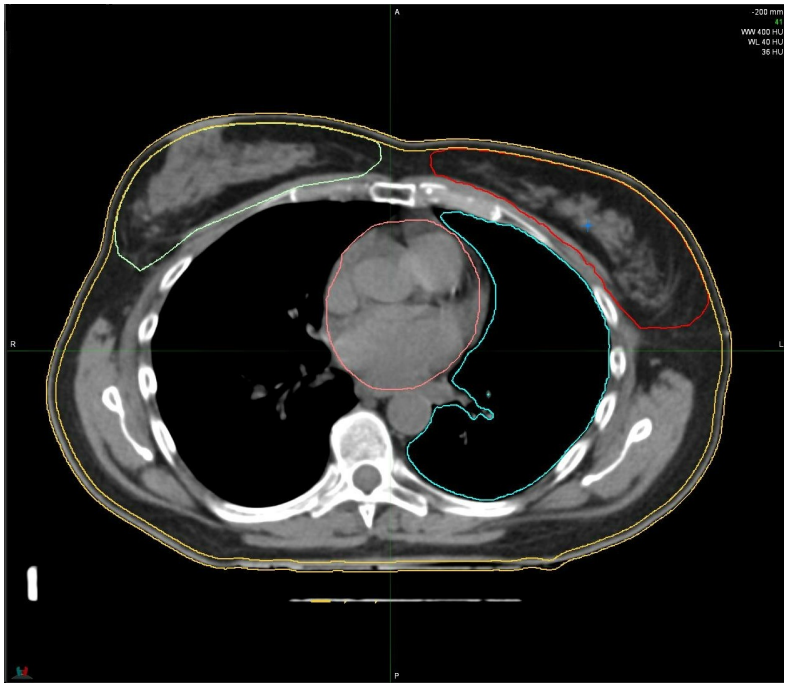

Figure 6: Example of the Skin contour (orange structure) generated through Mim Software.

Chapter 4

Results

A total of 1127 breast DICOM RT was retrieved from the original list of patients. We excluded 152 patients with incomplete dosimetric information, 32 patients with bilateral breast treatment, 11 patients treated with arc therapy and 2 patients that were treated with boost after a second clinical multidisciplinary visit. The ad-hoc designed MIM workflow processed the DICOM file to generate the "Skin" contour as presented in Chapter 3. The csv files with the absolute cumulative DVH were correctly generated for the whole sample with a processing time of 127 minutes. The dosimetric dataset was then merged with the treatment and clinical dataset collected by Fodor and colleagues, including the information on acute and late skin reactions and the cosmetic state recorded during the FU.

4.1 Dose Calculation Algorithms

Before the toxicity analysis, we performed an in-silico dosimetric study on a subgroup of 25 randomly selected patients (not considering patients using bolus). The study aimed to evaluate the differences among the dose algorithms rather than assess the more representative effective dose given to the 5 mm of the skin. We generated two equivalent treatment plans in addition to the approved one to compare the three algorithms currently available in the Eclipse TPS: PBC, AAA, and AXB. Three Skin DVHs were exported. The distribution of the average DVHs is depicted in Figure7 and 8. Focusing on PBC and AXB, the region between 5-15 Gy and 32-38 Gy were comparable (p-value > 0.05, table of p-value reported in Appendix C). The significant portions of the DVH calculated on 25 samples showed discrepancies generally less than 3-4% in percentage differences, values much larger than the corresponding inter-patient variability of DVH within our population. Based on these results, for the following analyses, we considered the DVH points greater than 5 Gy because of the inaccuracy of the algorithm (see

Figure7, but also to remove skin regions far away from the part of interest.

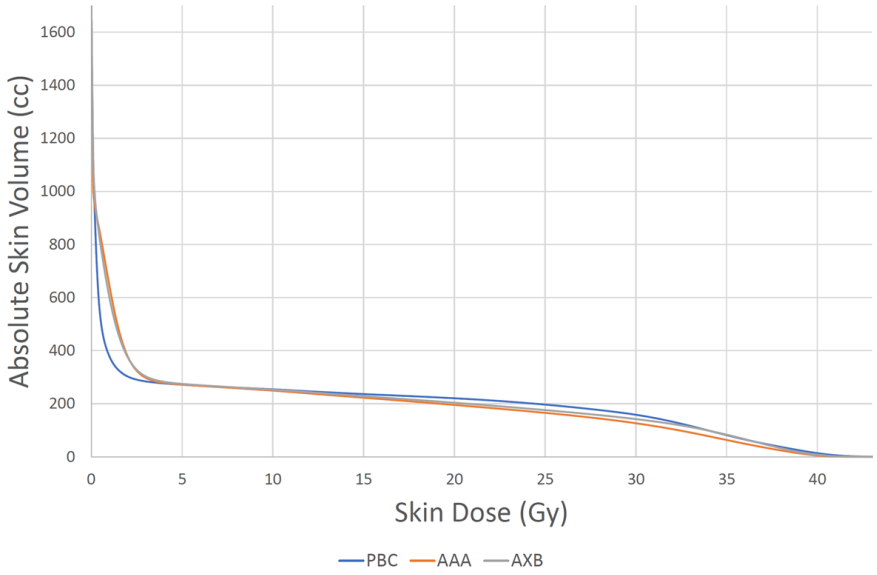

Figure 7: Comparison of the "Skin" DVH for the three Varian algorithms for dose calculation: Pencil Beam Convolution (PBC), Anisotropic Analytical Algorithm (AAA), and Acuros XB (AXB).

4.2 Acute Skin Reactions

Acute toxicity was assessed using the RTOG scoring criteria. One-hundred seventy patients representing 15.1% of the population reported G2+ toxicity (14.0% of G2 and 1% of G3 events), manifesting at least bright erythema, patchy moist desquamation or moderate oedema. Grade 1 was scored in 65.7% of patients. Average DVHs for patients with and without ACUG2 were shown in Figure 9, while in the Appendix C, we reported the p-value for t-test comparison. In univariate analysis, considering the entire population, significant associations were found for PTV volume, hypertension, diabetes, obesity, ALND, and V5-V20 Gy, V30 Gy and V34 Gy. Results are shown in Table 4.2.

Clinical Multi-variable model PTV volume was the best predictor, and it can be coupled with ALND in a pre-planning model for ACUG2 toxicity. Indeed, patients without ALND and small-average volume had a 12.5% of toxicity, the mixed group (large volume without ALND or ALND in patients with small-average volumes) had a rate of 18%, while the risk group represented by ALND and large

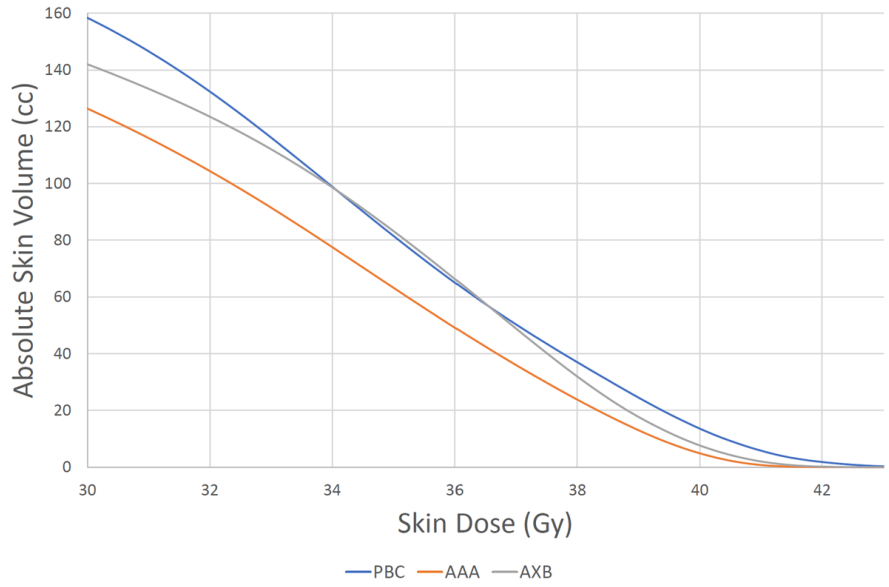

Figure 8: Details of the mid-high dose skin regions and differences between the algorithms. Pencil Beam Convolution (PBC), Anisotropic Analytical Algorithm (AAA), and Acuros XB (AXB).

volumes (more extensive than the third quartile) had 28% of ACUG2 toxicity. However, as expected, the average PTV volume for patients treated with bolus was lower than the opposite group (549 cc vs 749 cc, p-value, p-value 0.003 (check)), but due to the treatment technique, they experienced a larger toxicity rate (17.7% vs 14.4%, p-value 0.032 (check)). Consequently, to enforce the role of the volume in the preclinical model, we could include the bolus (yes/no) information (see Appendix C for model details).

Dosimetric Model Even if target volume was the best predictor, we defined a model including a dosimetric variable to identify possible dose-volume constraints; replacing the volume with dosimetric parameters has also the benefit to remove any dependence on CTV contouring and PTV generation. We could use V10-V15 Gy due to the previous considerations on the dose calculation. Moreover, they represented an advantage also in regarding the bolus application. Indeed, average DVHs shown in Figure10 highlighted that bolus patient, having a smaller volume, had lower histograms in the low-medium region of the DVH, with the bolus effect on DVH manifested in the mid-high dose region ($> 70\%$ of the prescription dose). Nevertheless, V10-V25 represented better descriptors than V30 and V34 Gy, indicating that individual volumes included in low-mid doses are correctly ranked independently from the bolus application.

Table 7: Logistic regression univariate analysis for early skin reaction of grade two or plus. We reported only significant factors with p-value ≤ 0.05.

Variable	**Coeff.**	**Std. Err.**	**z-score**	**P>z**	**OR**
PTV Volume (cc)	0.001	0.000	4.700	<0.0001	1.001
obesity	0.801	0.178	4.512	<0.0001	2.229
V5Gy	0.006	0.002	4.135	<0.0001	1.006
V10Gy	0.007	0.002	3.928	<0.0001	1.007
V15Gy	0.007	0.002	3.828	<0.0001	1.007
V25Gy	0.008	0.002	3.813	<0.0001	1.008
V20Gy	0.007	0.002	3.766	<0.0001	1.007
Median PTV Volume (913cc)	0.632	0.171	3.696	<0.0001	1.882
V30Gy	0.008	0.002	3.549	<0.0001	1.008
3rd Quartile PTV Volume (642 cc)	0.474	0.182	2.604	0.009	1.607
ALND	0.478	0.196	2.440	0.015	1.613
V34Gy	0.006	0.003	2.250	0.024	1.006
Diabetes	0.655	0.301	2.177	0.029	1.925
Hypertension	0.355	0.170	2.086	0.037	1.427

For practical and historical reasons, we decided to use V20 in the following cases where we have to define a dose-constraints for the plateau region of the DVH, representing the treated volume, similarly to the practice of considering the fraction of organ within the fields (i.e.: in the original tangential field irradiation, corresponding to the 50% of the prescribed dose). For ACUG2, we developed a final model with ALND, V20 and obesity, with this last factor suggesting possible non-manifested health comorbidities, dysfunctions or different tissue compositions. Table 4.2 reports statistical values, area Under the ROC Curve (AUC), and calibration results with slope and intercept were 0.61, 1.02 and -0.004, respectively. Figure11 represents the dose-response curves for the model. In the whole population, we registered a partial consequentiality with 10% of the acute tox patients experiencing EH at six months (chi square p-value = 0.0003) and 10.1% late fibrosis within the 42 months after the end of RT (chi square p-value < 0.0001.
Associations between post-surgery conditions and acute symptoms were not identified. Consequently, we did not perform further analysis considering such information as a surrogate of the baseline toxicity.

Patients treated without Bolus The subgroup consisted of 878 patients with a rate of ACUG2 equal to 14.4%. Differently from the previous case, we could identify a three-variate preclinical model, including PTV volume, ALND and hypertension (AUC = 0.64, see Appendix C for statistical details).
Three dosimetric models were developed using V20 Gy and two factors between hypertension, obesity and ALND. AUC was comparable between the models; the

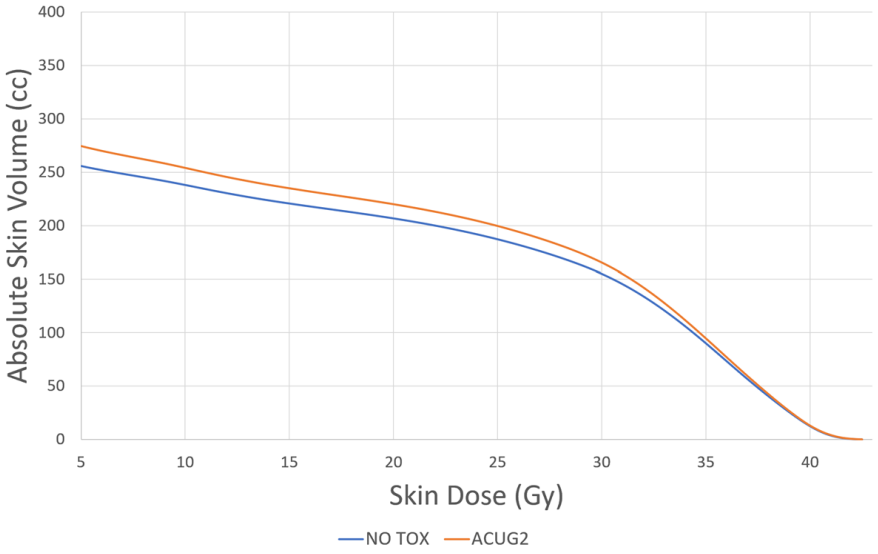

Figure 9: Average DVHs for patients experiencing or not early skin reaction of grade 2 or plus.

best value (0.64), supported by the highest p-value for Hosmer & Lemeshow test, was found in V20 Gy, obesity and hypertension.
As previously tested, 11.1% of patients with acute reactions developed EH, while 12.7% flowed in FATP.

Patients treated with Bolus For this group of patients, 44/250 patients manifested ACUG2 after RT. In the univariate analysis, age (protective factor), tamoxifen therapy, aromatase inhibitor (protective factor), PTV95% (protective factor) and PTV volume. The latter factor showed a substantial reduction in the significance (p-value 0.053) compared to the previous analysis. However, it gained importance when coupled with age as a protective factor (see Appendix C for details). No dosimetric variable was found as a descriptor for ACUG2 in the bolus population. Interestingly, the acute toxicity affected by the bolus application did not flow in chronic symptoms, with 1/44 (2.4%) of acute toxicity becoming a FATP, while 3/44 (6.8%). Moreover, the ALND exited from the list of significant variables in the bolus group even if the presence of ALND in the non-bolus and bolus group is the same (18.6% vs 18.5%).

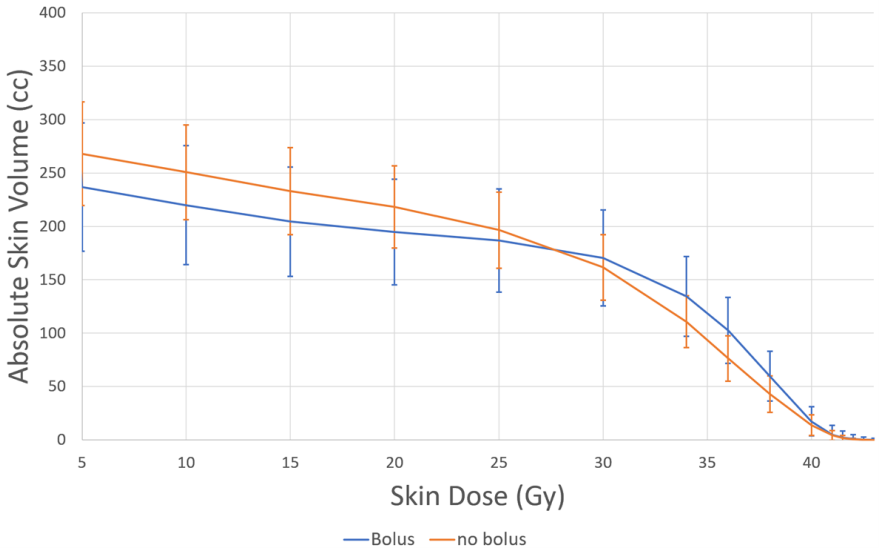

Figure 10: Average DVHs for patients treated with and without bolus application. Effective DVH points were reported with error bars.

4.3 Oedema-Hyperpigmentation Analysis

The early-late skin reactions such as Oedema and Hyperpigmentation were assessed considering the results by Fodor[33] that showed an incidence plateau for EH after six months. A total of 52 (4.6%) over 1118 patients with six months FU experienced G2+ marked or generalized hyperpigmentation or moderate localized oedema, and intervention indicated or limited instrumental Activity of Daily Living (ADL). Average DVHs for the endpoint are depicted in Figure 12. P-value from statistical t-test are included in the Appendix C. The separation between the DVH points is larger than in the ACUG2 case. In univariate analysis, we found associated factors: PTV volume, V15Gy, V20Gy, V25Gy, V30Gy, V34Gy, ALND, ACUG2, Body D1, obesity and chemotherapy. PTV V95 (risk factor), hypertension, bolus (protective factor) and age (in continuous, as a risk factor) were slightly over the significance threshold. Statistical values are reported in Table 8. Consequently, this analysis was performed without differentiating between bolus and non-bolus patients. Thirty-three per cent (17 patients, chi square p-value = 0.0003) of patients with G2+ EH had previous acute reactions, while 26% (13 patients, chi square p-value < 0.0001) will also develop FATP. The relative DVH points showed a protective behaviour suggesting that for such symptoms, the absolute value of the irradiated volume is more relevant than its proportion with the organ structure.

Table 8: Univariate analysis for Edema and Hyperpigmentation grade 2 or plus, including factors with p-value below 0.05.

Variable	**Coeff.**	**Std. Err.**	**z-score**	**P>—z—**	**OR**
PTV Volume (cc)	0.002	0	5.557	<0.0001	1.002
3rd Quartile PTV Volume (642 cc)	1.48	0.289	5.125	<0.0001	4.392
V15Gy	0.014	0.003	4.941	<0.0001	1.014
V20Gy	0.015	0.003	4.903	<0.0001	1.015
V5Gy	0.011	0.002	4.871	<0.0001	1.011
V25Gy	0.015	0.003	4.648	<0.0001	1.015
ALND	1.159	0.294	3.945	<0.0001	3.188
V30Gy	0.013	0.003	3.866	<0.0001	1.013
Median PTV Volume (913cc)	1.183	0.326	3.629	<0.0001	3.264
AcuG2	1.065	0.308	3.456	0.001	2.902
BodyD1NEW	1.059	0.328	3.233	0.001	2.884
Obesity	0.938	0.29	3.232	0.001	2.554
V34%	-7.903	2.521	-3.135	0.002	0
V36%	-8.612	2.999	-2.871	0.004	0
V38%	-11.134	4.442	-2.507	0.012	0
V34Gy	0.009	0.004	2.325	0.02	1.009
V34 Quartile	0.663	0.294	2.255	0.024	1.94
Chemio	0.577	0.291	1.985	0.047	1.781
PTV V95(%)	0.188	0.098	1.916	0.055	1.207
Hypertension	0.529	0.286	1.853	0.064	1.698
Age	0.023	0.012	1.843	0.065	1.023

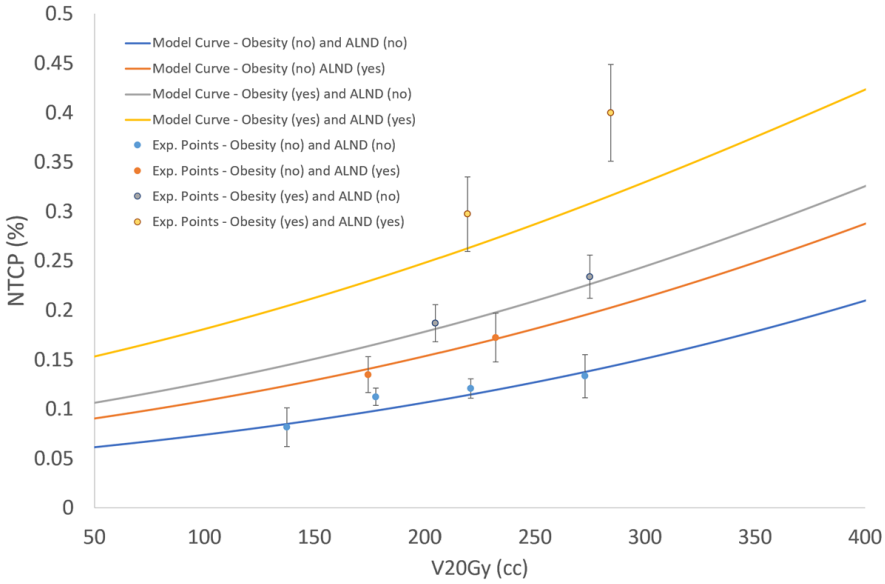

Figure 11: Dose-response relationship for early skin reaction grade 2 or plus as a function of Skin Volume receiving 20 Gy.

Clinical Multi-variable model As expected, ALND resulted strongly associated with the EH endpoint. The first model we developed was similar to the one for the acute endpoint. In this case, both the factors had a larger coefficient than in the ACUG2 case, AUC was 0.75, but the calibration slope was poor with a slope of 0.89 (see Appendix C for further details).

Dosimetric Model The attempt to substitute the target volume with a dosimetric descriptor was performed using V20 Gy again. V20Gy aimed to consider the bolus effect in the dosimetric variable for this endpoint. As in the ACUG2 case, ALND entered the model with the dosimetric variable and an OR of 3.11. AUC was comparable with the previous model (0.74), same for the calibration slope (0.87), but the HL p-value was larger for the clinical model, suggesting a better goodness of fit (0.64 vs 0.54).

Patients without bolus For this class of patients, 46 (5.3%) G2+ EH events were recorded among 870 people. As reported in Appendix C, V30, V34, V36 Gy, chemotherapy, Body D1 and hypertension improved their significance compared to the whole population. The median wait time between the surgery and RT was a predictor of EH (patients treated before and after 77 days from the surgery). Cosmesis factors in the univariate analysis showed a p-value of around 0.10, suggesting its possible role as a baseline toxicity surrogate. We developed the

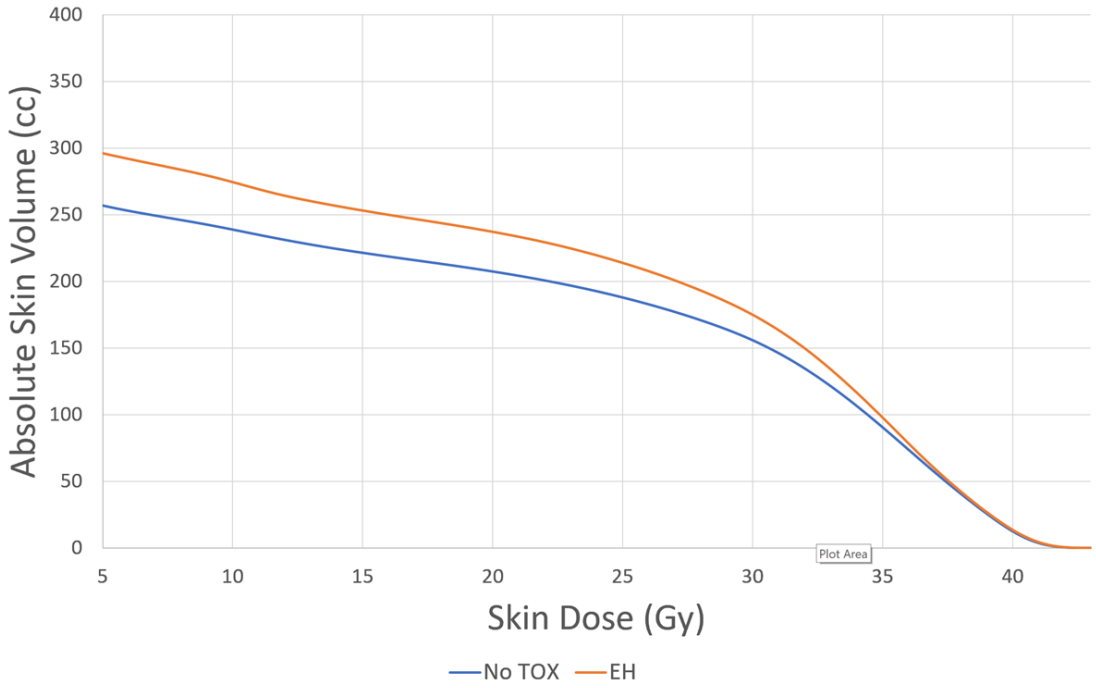

Figure 12: Average absolute skin DVHs for patients with or without Edema-Hyperpigmentation grade 2 or plus.

same models for the subgroup of patients without bolus application with a slight improvement in the AUC (1%) and a more calibrated plot with 0.92 and 0.93 in slopes for pre-planning and dosimetric cases. Patients with bolus application A limited statistical power characterized the group of patients treated with bolus application with 6 events over 250 patients. Volume was the only significant factor, and ALND was no anymore significant.

4.4 Fibrosis-atrophy-telangiectasia-pain Analysis

According to the findings by Fodor and colleagues, the incidence of FATP increased with time. We evaluated the rate of events at 42 months vs 54 months prior to the coupling with the dosimetric information. The rate was comparable with 45 events over 1242 patients (3.6%) and 35 over 995 patients (3.5%), respectively, but we lost some patients due to the FU time; consequently, we reasonably placed the time threshold at 42 months. After joining the dosimetric dataset of the "Skin" DVHs, the rate for FATP G2+ was 3.8% with 40/1066 patients. Among them, 32% had EH before FATP, while 40% manifested ACUG2. Average DVHs for

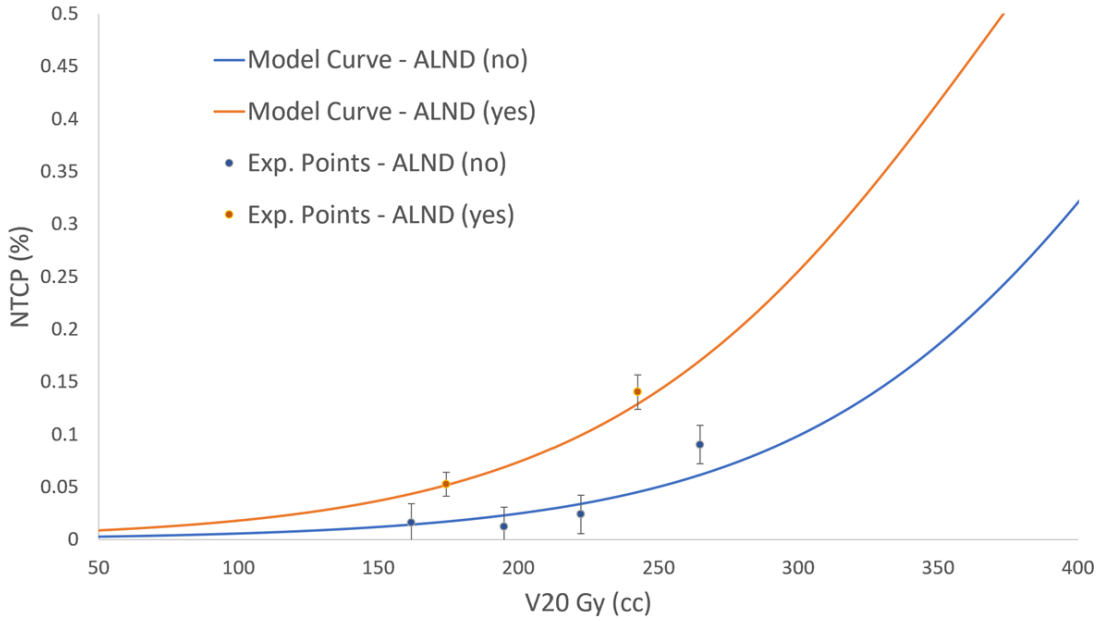

Figure 13: Dosimetric model for oedema and hyperpigmentation grade 2 or plus calculated on the whole population of breast cancer patients.

FATP G2+ are shown in Figure 14. The DVHs separation between patients with and without FATP G2+ was larger than the acute and early-late endpoints.
In univariate analysis, we found: PTV volume, Cosmesis post-surgery, all the DVH points from previous EH G2+, previous ACUG2, and aromatase inhibitors (protective factors). The number of segments, third quartile for PTV hotspot (PTV V105%), hypertension, ALND, 9+ fractions of bolus, in situ histology, and RT treatment time had a p-value between 0.05 and 0.08 (Table 9).

Clinical Multi-variable model A more complex model was built for FATP. It included PTV Volume, ALND (with a gain in the logistic coefficient value), and Aromatase Inibhitors as a protective factor. Moreover, we included the multivariate model of the cosmetic variation after breast surgery to measure possible effects not directly derived from ionizing radiation. In Table 4.6 are reported coefficients and statistics for the four-variable model, AUC was 0.82 and calibration slope 0.96 (further details in Appendix C).

Dosimetric Model We proposed a dosimetric model that considers the volume at the plateau of the dose distribution (V20 Gy) and the effect of the high dose on a small region (V42Gy, 105% of the prescription dose). This choice comes from

Table 9: Univariate analysis for fibrosis-atrophy-telangiectasia-pain grade 2 or plus, including factors with p-value below 0.05.

Variable	**Coeff.**	**Std. Err.**	**z-score**	**P>—z—**	**OR**
Oedema G2	2.555	0.377	6.780	0.000	12.870
PTV Volume (cc)	0.002	0.000	5.773	0.000	1.002
Cosmesis	1.930	0.360	5.355	0.000	6.892
V5Gy	0.013	0.003	4.908	0.000	1.013
V15Gy	0.015	0.003	4.791	0.000	1.015
V20Gy	0.016	0.003	4.692	0.000	1.016
V25Gy	0.016	0.004	4.567	0.000	1.016
AcuG2	1.415	0.335	4.223	0.000	4.117
V30Gy	0.015	0.004	4.099	0.000	1.015
3rd Quartile PTV Volume (642 cc)	1.230	0.325	3.787	0.000	3.422
Obesity	1.181	0.326	3.628	0.000	3.258
V34%	-11.891	3.329	-3.571	0.000	0.000
V34Gy	0.013	0.004	3.154	0.002	1.013
V38Gy	0.017	0.006	3.148	0.002	1.018
V41Gy	0.050	0.017	3.003	0.003	1.051
V36Gy	0.013	0.004	2.975	0.003	1.013
BodyD1NEW	1.073	0.361	2.967	0.003	2.923
V40Gy	0.029	0.010	2.894	0.004	1.030
V41.5Gy	0.072	0.025	2.862	0.004	1.074
Median PTV Volume (913cc)	0.929	0.351	2.651	0.008	2.533
V42 Gy	0.107	0.041	2.650	0.008	1.113
V36%	-8.447	3.387	-2.494	0.013	0.000
V425	0.198	0.083	2.375	0.018	1.219
Aromatase Inhibitor	-0.637	0.329	-1.936	0.053	0.529
Num. of Segments	0.194	0.101	1.921	0.055	1.214
PTV V105 3rd quartile (in cc)	0.627	0.335	1.874	0.061	1.872
V34 Quartile	0.622	0.335	1.859	0.063	1.862
Hypertension	0.589	0.323	1.820	0.069	1.802
ALND	0.641	0.354	1.809	0.071	1.898
More than 9 fr of Bolus	1.137	0.632	1.799	0.072	3.119
In situ ductal carcinoma	0.579	0.324	1.788	0.074	1.785
RT days	0.063	0.036	1.726	0.084	1.065

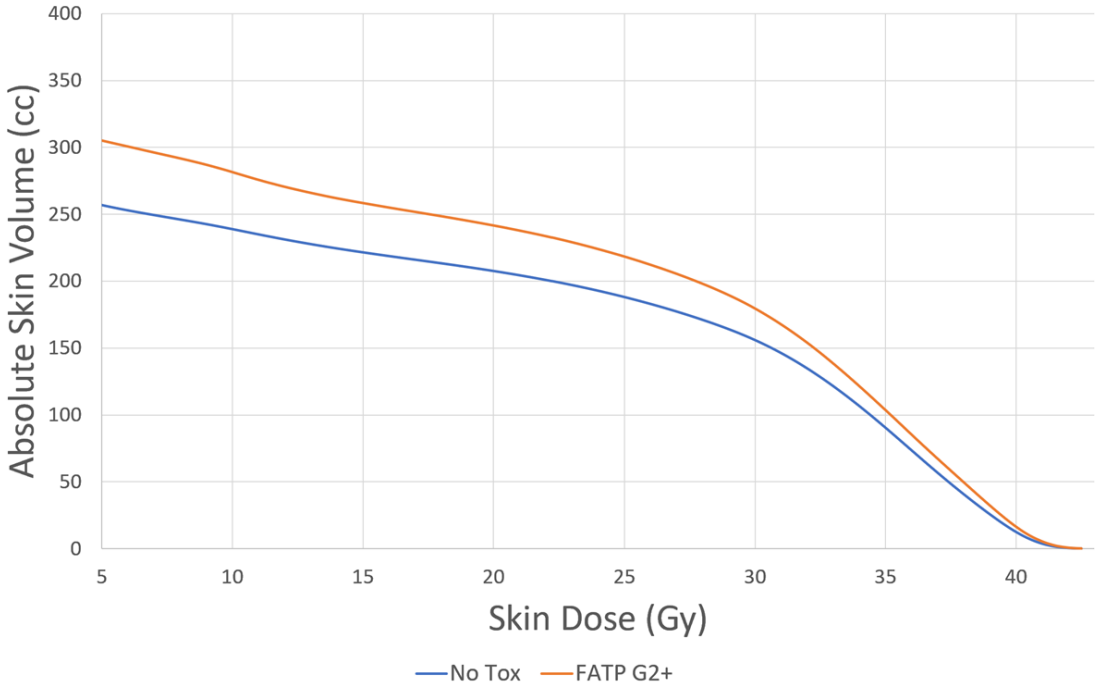

Figure 14: Average DVH points for fibrosis-atrophy-telangiectasia-pain symptoms of grade 2 or plus.

the literature on the importance of the hotspot for FATP-like side effects. Indeed, such behaviour was confirmed in the studied population through V105% quartile and the significance of DVH points in the tail of the histogram. Table 4.7 describes the statistical parameters for the five-variable model. Predicted curves and experimental points are reported in Figure 4.9. For graphical reasons, we were forced to apply some simplification of the model. First, we transformed the V42 Gy in a binary variable with values below and over 2 cc as a cutoff. Secondly, we reported in the plot only the curves with a single risk/protective factor, the standard curve (represented by patients without ALND, aromatase inhibitor drugs, cosmetic alteration and with low values of V40), and the curve for the class of patients with the highest risk of developing FATP G2+.
On top of this model, delay in the treatment was found to be a risk factor. The odd ratio was 1.08 for every day of postponement of the treatment end or 10.8 for patients with a treatment duration longer than 25 days. Apparently, delay in the treatment could happened due to the acute toxicity development, nevertheless, correlation between days of treatment and ACUG2 was not present (r=0.02, P=0.46). Finally, we did not perform a subgroup analysis for this endpoint for statistical limitations.

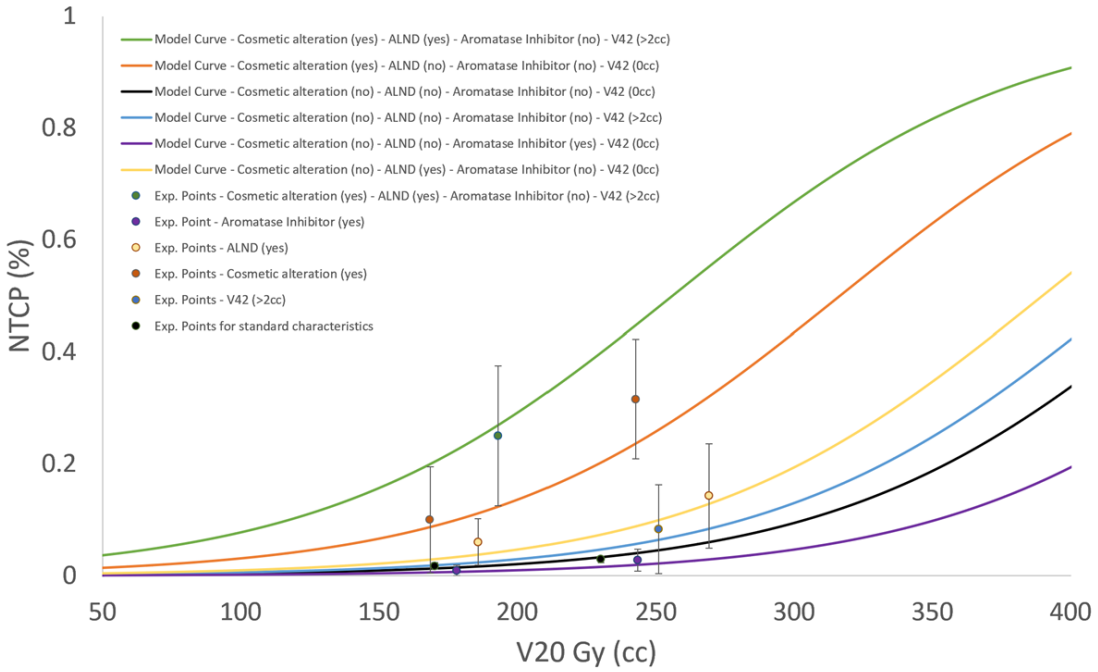

Figure 15: Dose-response relationship for a multivariate model describing for fibrosis-atrophy-telangiectasia-pain grade 2 or plus.

4.5 Liponecrosis Analysis

Liponecrosis was recorded in 118 patients, that is, 10.5% of the whole population. The average DVHs for patients with and without symptoms are shown in Figure 4.10. In univariate analysis, there was some clear evidence for this endpoint. We studied the subgroup of patients without bolus application due to the negligible presence of this symptom with the increase of the bolus fraction number (1.6% in patients having more than 7 bolus fractions). The new rate is 10.9%, with 96 events on 878 patients. V30Gy was the first dosimetric factor; no dosimetric factors were found over 34 Gy. Moreover, V30 Gy and Target V95% (risk factor) were more relevant than Target volume. PTV V105% was controversially protective, possibly due to its relationship with V95%, suggesting that for such symptoms, the dose to a large volume is more important than dose hotspots. From the clinical side, chemotherapy and monoclonal antibody treatments were found as risk factors, while the endocrine-therapy was a protective factor. The same behaviour was found for the age (threshold over the quartile,i.e. 65 years old). Statistical values are reported in Table 4.5.

A multifactorial model was developed, including hormone therapy, V30Gy to

Table 10: Univariate results from logistic regression for breast liponecrosis.

Variable	**Coeff.**	**Std. Err.**	**z-score**	**P>z**	**OR**
V30Gy	0.009	0.003	2.842	0.004	1.009
V25Gy	0.008	0.003	2.818	0.005	1.008
PTV V95(%)	0.205	0.074	2.764	0.006	1.228
V20Gy	0.007	0.003	2.725	0.006	1.007
median PTV Volume (913cc)	0.624	0.232	2.696	0.007	1.867
PTV Volume (cc)	0.001	0.000	2.657	0.008	1.001
V15Gy	0.006	0.002	2.629	0.009	1.006
V5Gy	0.005	0.002	2.616	0.009	1.005
3rd Quartile PTV Volume (642 cc)	0.571	0.226	2.522	0.012	1.770
V34Gy	0.009	0.004	2.416	0.016	1.009
V105	-0.661	0.279	-2.372	0.018	0.516
Chemotherapy	0.517	0.226	2.290	0.022	1.678
Age (>= 65 yo)	-0.598	0.275	-2.171	0.030	0.550
Hormone Therapy	-0.533	0.248	-2.148	0.032	0.587
V34%	-4.485	2.114	-2.122	0.034	0.011
Monoclonal Antibodies	0.650	0.317	2.049	0.040	1.915
V36%	-5.114	2.670	-1.915	0.055	0.006
V36Gy	0.008	0.004	1.815	0.070	1.008
In situ ductal carcinoma	0.379	0.217	1.746	0.081	1.460

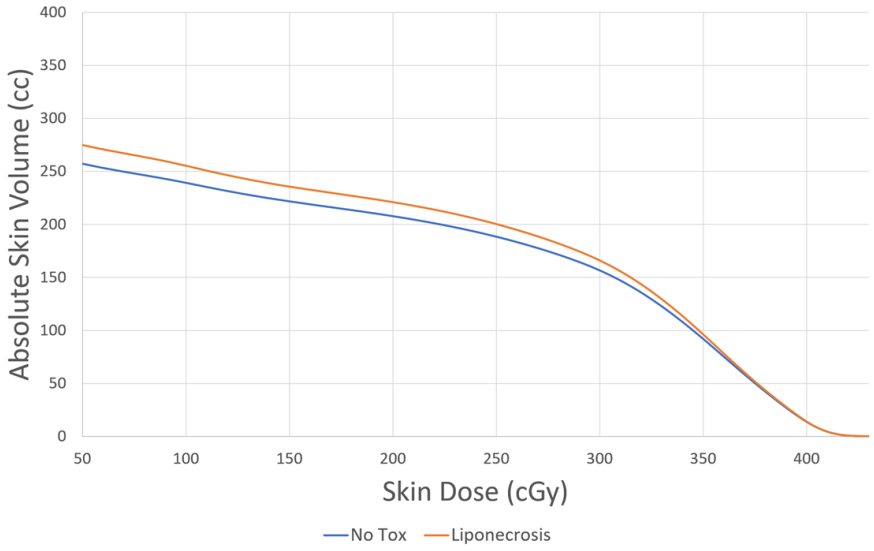

Figure 16: Average DVH points for experiencing or not Liponecrosis in the breast.

the skin and patients' age ($\geq$ 65 years old). PTV coverage could also be included, but we present a model without this factor. In any case, it would result included more like a fact than a variable of action; it is for the patients' age, both can impact the reduction of the V30 value to maintain the liponecrosis below acceptable clinical levels. Statistical characteristics are reported in Table 4.8. Dose-response relationships for the model are reported in Figure 17. Due to the similar OR for the age and endocrine therapy, we reported two model curves to represent the slight differences graphically. However, then we computed a single group of experimental rates for such a combination of patients, i.e., patients younger than 65 years old with hormone therapy and patients older than 65 years old without any assumption of hormone drugs.

Table 11: Multivariable Dosimetric Models for the studied endpoints

NTCP Model for Acute Toxicity					
AUC = 0.61 calib = 0.00 + 1.02 x, HL p = 0.85					
Variable	Coeff.	Std. Err.	z-score	P>z	OR
ALND	0.419	0.199	2.101	0.036	1.520
Obesity	0.598	0.199	3.004	0.003	1.818
V20 Gy	0.004	0.002	2.069	0.039	1.004
Constant	-2.926	0.448	-6.535	0.000	0.054

NTCP Model for Oedema and Hyperpigmentation					
AUC = 0.74 calib = 0.01 + 0.87 x, HL p = 0.64					
Variable	Coeff.	Std. Err.	z-score	P>z	OR
ALND	1.136	0.299	3.794	0.000	3.114
V20 Gy	0.015	0.003	4.783	0.000	1.015
Constant	-6.591	0.743	-8.866	0.000	0.001

NTCP Model for Fibrosis-Atrophy-Telangectasia-Pain					
AUC = 0.82 calib = 0.00 + 0.96 x, HL p = 0.40					
Variable	Coeff.	Std. Err.	z-score	P>z	OR
ALND	0.819	0.376	2.179	0.029	2.267
Aromatase Inhibitor	-0.779	0.348	-2.236	0.025	0.459
Cosmesis	1.951	0.385	5.074	0.000	7.038
V20 Gy	0.016	0.003	4.561	0.000	1.016
V42 Gy	0.086	0.045	1.940	0.052	1.090
Constant	-7.004	0.866	-8.088	0.000	0.001

NTCP Model for Liponecrosis					
AUC = 0.63 calib = 0.00 + 0.98 x, HL p = 0.49					
Variable	Coeff.	Std. Err.	z-score	P>z	OR
Hormone Therapy	-0.554	0.251	-2.211	0.027	0.574
V30GY	0.010	0.003	3.011	0.003	1.010
Age ($\geq$ 65)	-0.492	0.230	-2.141	0.032	0.611
Constant	-2.990	0.551	-5.426	0.000	0.050

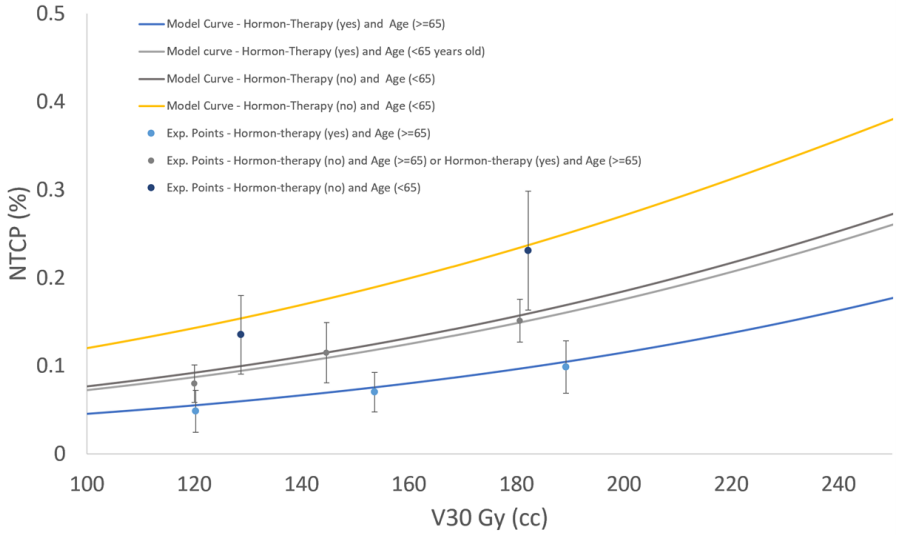

Figure 17: Dose-response relationship for the multivariate model describing breast liponecrosis.

Chapter 5

Discussion

In this study, we developed four dosimetric models for acute and late skin reactions on a population of 1128 early-stage BCa patients with a median FU of 72 months. The size of the studied cohort and the quality of the data collected during so long time represent two strong point for the robustness of the resulting NTCP models. Moreover, the study focused on the relationship between skin alterations and the dose individually delivered to the patients "Skin". The use of skin structures has already been proposed in other districts [52], but it is the first time it has been addressed RT for BCa. Specifically, we decided to investigate three different toxicity domains: acute skin reactions, the superficial manifestation of oedema-hyperpigmentation, fibrosis, atrophy telangiectasia and pain as a group of moderate-severe cutaneous and subcutaneous symptoms in the late phase. In addition, we investigated in the late time the development of fat necrosis with associated dystrophic calcification.

PTV Volume The first feature not directly related to the dosimetry of the patient and common to the four endpoints was the PTV volume. As reported in Table 2.4, breast volume or surrogates correlated with acute and late skin reactions in many populations studies despite the different cohort characteristics [51, 48, 7, 8, 45, 61, 44, 35, 16]. The most acknowledged reasons are the presence of hotspot regions in patients with large target volumes or, likely more reasonable, the larger amount of skin irradiated, reducing the repair capacity. We have, infact, previously discussed the possible relationship with the damage to the FSUs, the importance of the absolute irradiated volume (instead of considering the relative DVHs), the presence of other comorbidities affecting the peripherical circulation, and the tissue composition. It is reasonable to believe that the answer to the relationship between volumes and toxicity resides in all of the mentioned aspects. This could explain its correlation with both acute and late, cutaneous and subcutaneous symptoms. For example, in our population, the link between PTV Volume and PTV V105(cc) is

not supported by clear correlation (see the plot in Appendix D), and consequently, for most of the endpoints, the PTV Volume was the first covariate, but hotspot were not found as a significant risk factor. Toxicity rates for volume quartile groups were reported in Appendix C, with EH and FATP representing differences of 2.5-3 times for patients with mid-high volumes (from II to III quartile, EH = 3.5%, FATP = 3%) and high volumes (larger than IV quartiles, EH = 10.9%, FATP= 7.9%).

Other factors associated with skin reactions We were able to identify four treatment factors (lymph node dissection, aromatase inhibitor, hormone therapy, surgery impact on breast cosmesis) and two patients' features (obesity and age) affecting the development of acute and late skin reactions.
Axillary lymph node dissection was found as a risk factor in acute and late endpoints, confirming the importance of lymphatic vasculature in regulating the inflammatory response. Indeed, the lymphatic system influences the drainage of extravasated fluid, inflammatory mediators, and leukocytes having a strong relationship with oedema formation (toxicity rates three times the ones observed in sentinel lymph node dissection [84]). Regarding the other endpoints, Torres and colleagues [78] have proved through ultrasound measurements that axillary dissection increased breast skin thickening during and 6 weeks post-RT, with more considerable variations associated with higher toxicity severity. Lin et al. [49] confirm the result with the long-term impact still visible at 1 year after the RT completion.
We have already discussed the role of obesity, which entered in the acute model together with the dosimetric variable representative of the PTV volume. Two possible explanations for this variable can be hypothesized; first, the importance of the health condition (precisely, proper vascular functionality) beyond the radiobiological and physics explanation of the large breast volumes; then, the role of fat sensitivity to radiation. Although there are studies suggesting the use of fat graft as protective for radiotherapy treatments, it is also investigated the relationship between adipose tissue delivered with radiation and the development of fat and the development of cardiometabolic disease impacting both clinical and toxicity outcomes[42].
Regarding the aromatase inhibitor, the analysis by Kraus [45] highlighted a risk factor for moderate erythema, which is supported by the evidence of cutaneous vasculitis following the use of this estrogen blocker citesantoro. Our results showed a protective role for aromatase inhibitor, which is in contrast with the positive role of estrogen for skin thickness, elasticity and hydration since targeted estrogen replacement could be administrated for long-term skin management in postmenopausal women[72].

Endocrine treatment was associated with liponecrosis, confirming the findings in the literature of a positive impact of hormone replacement therapy on fat distribution within the tissues[73, 77, 58, 46]. In conclusion, we introduced for the late endpoint the presence of cosmetic alteration following the conservative breast surgery as a way to take into account the tissue damage induced by a surgical intervention which cooperates with the radiation insult to the formation of fibrosis, atrophy and pain.

Skin DVH points The risk associated with large breast volume is an important aspect that must be considered in managing the WBI after BCS. Patients with wide breasts must be followed with more attention, and medical intervention through creams must be prepared to protect them from dermatitis and relieve skin irritation. Nevertheless, NTCP modelling aims for a more active role in managing tissue reactions, which is why, in this study, we moved to the dose-response relationship from the DVH of the "Skin". We observed separations along the entire average DVHs for patients with and without toxicity for all four endpoints, suggesting that patients with more large PTV volume have higher DVH points without a planning intervention. Reasonably, due to this strong impact on the breast volume, we found the DVH points more correlated to the PTV volume as a significant factor. We decided to use the V20 Gy (50% of the prescription dose) as the volume factor from the DVH. For anatomical and physical reasons, the ranking of patients by V20Gy is similar along all the plateau (V10 Gy to V30 Gy, correlation with PTV volume ranging from 0.87 to 0.60), suggesting that any choice within this range can be applied without visibly impacting on the results. Nevertheless, we have tested that in the DVH tail (we analyzed V36 Gy representing the 80% of the prescribed dose), there are moderate and large changes in the position of the patients' ranking compared to the list computed at V20 Gy. Thus, there is space for applying dosimetric precautions in the last part of the DVH, whatever the patient's target volume. Consequently, when applicable, we tried to combine in our model the volume DVH factor (V20Gy) and a DVH point coming from the tail of the histogram. Importantly, using V20 in place of the PTV volume permits to apply this predictor independently of the methodology of contouring CTV and generate PTV, making the corresponding models better generalizable compared to the ones based on breast volume/PTV. And, of course, it translates into a model radiobiologically interpretable in terms of FSU and skin volume/surface threshold for a relevant increase of the risk, according to the classical behaviour of skin toxicities insurgence.
For moderate-severe acute toxicity, we observed separation between the two average DVHs with p-values at univariate always smaller toward the end of the histogram. Consequently, we identified a three-variate model for this endpoint,

including V20Gy as a dosimetric factor and lymph node dissection and obesity as clinical factors. According to the model, a constraint on V20 Gy for controlling the risk of ACUG2 below a threshold of 15% can be identified (i) at 295 cc for patients without any risk factors, (ii) at 190 cc for patients with ALND, (iii) at 150 cc for obese patients, while for the highest risk group (ALND and obesity) we can apply a constraint of 200cc for an ACUG2 risk below 25%.
We developed a bivariate model with V20 Gy and lymph node dissection for oedema-hyperpigmentation toxicity. The more clear average DVH separation between patients with and without symptoms is reflected in a larger dosimetric weight in the NTCP model (OR=1.014 for EH vs OR=1.004 for ACUG2). Moreover, lymph node dissection showed a more substantial relation with EH toxicity, with a doubling in the OR (from 1.51 to 3.11). From the NTCP model, we could identify V20Gy< 250 cc for an EH risk below 5% for patients without ALND. In the ALND group, we could apply a constraint of 220 cc for the risk of EH below 10%.
The liponecrosis was described through a three-variable model with V30Gy representing the best dosimetric descriptor. The other factors were age (over 65 yo as a protective feature) and endocrine treatment (as a protective factor), with similar impacts on the reduction of the probability risk. The constraint we identified for risk of such subcutaneous alteration below 10% were V30 Gy< 180 cc for patients treated with hormone and elder than 65 yo, V30Gy< 130 cc for the mixed classes (age 65+ and no hormone therapy, patients younger than 65 yo and with endocrine therapy) and V30Gy< 125 cc (NTCP¡15% instead of 10%).
The NTCP model for FATP included five factors: two dosimetric factors representing the plateau, (i) V20Gy, and the tail of the DVH, (ii) V42Gy, two clinical factors, the (iii) aromatase inhibitor as a protective factor and (iv) ALND with the same behaviour expressed in the other endpoints, and the (iv) cosmetic condition after the surgery as a possible feature expressing a baseline impairment due to the surgical procedure. Interestingly, for this endpoint which also included subcutaneous reactions, we were able to identify a dose relationship for the "Skin". At this level, it is still not clear if this is only an indirect correlation of breast volume or to the dosimetry of other more directly involved structures. A validation study confirming these dosimetric findings could drive in identifying the proper constraints and the impact of the 5 mm tissues in the acute and late skin reactions. Indeed, to proceed in the identification of robust NTCP models, a validation study is currently ongoing on the REQUITE population[70]. The analysis will be performed on the subgroup of 428 patients with treatment characteristics similar to the present study cohort (40-42.5 Gy in 15-16 fr and without the dose boost).In case of positive results, the validation will be extended to the 50 Gy in the 25 fr group (other 165 patients).
As already discussed, the advantage of the inclusion of skin contour into the breast

RT protocol represents a possible active way to manage the risk of developing acute and late skin symptoms through plan optimization; this potential is not offered by the PTV volume and the PTV DVH points (excepting the hotspot concept). Reasonably, the "window" of intervention for such an organ is more limited than other structures since the skin embeds part of the tumour and also because of the physical restriction of a tangential treatment. Nevertheless, we have shown that without any planning rules for the skin, there were patients with similar volume for V20 Gy but differences in the V36 Gy (see Appendix D), suggesting that there is chance to control the "Skin" dosimetry without compromising the PTV coverage. To further support this hypothesis, we reported in Appendix D the scatter plot for V10-V36Gy against the Target Volume, where the linear fit showed an absence of correlation between the V36Gy distribution and the PTV volume. From this point of view, the tangential-like IMRT with the inverse-planning approach should represent the most appropriate way for a clinical application of such models. Although in a different district, the Head&Neck, Lee et al. already tested this possibility with the aim of reducing skin necrosis after radical RT. Figure 5.1 shows the exciting impact on the DVHs when the skin is included as a sensitive structure in the planning. A simulation of the feasibility of the planning intervention will be performed on a small cohort of BCA patients; the original plan will be compared with a tangential IMRT plan, a FIF plan with the addition of a field closed (field weight$>$ 0.5) on the external side of the PTV and an hybrid approach with partial arc irradiation. Our institution has recently introduced the ViTAT (Virtual Tangential-fields Arc Therapy), mimicking tangential field irradiation for whole breast radiotherapy. A dosimetric comparison of the PTV and the OARs has been performed with positive results both for left and right breast treatment[32]. Then, proper modelling of the ViTAT clinical plans was implemented through the knowledge-based (KB) approach implemented in the Eclipse™ Varian System, the Rapid Plan (RP), introducing the possibility of replacing manual planning with automatic ViTAT planning. As a very preliminary exploration, we applied the MiM workflow for generating the "Skin" in a subgroup of 5 patients from the dosimetric comparison study by Esposito et al. study. In this way, we could extend the analysis between standard tangential field and ViTAT also on this structure. The first results showed a promising advantage of the ViTAT for all of the considered patients and along the entire DVH. The study will be extended to understand which part of the Skin DVH is more prone to dosimetric reduction in the planning phase. These preliminary results suggests that in selected patients, modifications of the treatment technique using partly blocked (or unblocked) arcs may be of benefit in terms of potential reduction of skin toxicity despite this may be considered with caution considering any possible underdosing of PTV.

We have already highlighted the strength of the current study, but it is worth mentioning again in the Discussion the limitations that we have encountered during the analysis. The study analyzed four endpoints of acute and late skin reactions, but we did not have any information on the patient toxicity status before the RT started. Even though this is not a big issue for liponecrsis and FATP analysis, it can be a confounding factor for acute toxicity and EH symptoms, which can be more affected by the side effects coming from the BCS. In the analysis, we explored other clinical evaluations as possible surrogates for the patients condition before the RT. For example, in the FATP, we included the cosmetic state as a risk factor associated with the surgery. Another factor creating noise in the analysis was the evolution of the dose calculation system at our institute in the years of the patient enrollment. Differences between PBC, AAA, and AXB, in our treatment setting, were reported in a preliminary analysis shown in Chapter 4, and showed a better concordance for PBC and AXB, i.e. the ones covering the 99% of our study treatments. Unfortunately, we could not differentiate the analysis between the two groups of patients since the information on the dose calculation algorithm is not reported in the DICOM file. A new analysis, applying a temporal threshold for discriminating between DVH coming from PBC and AXB, will be performed in the future to assess if there are variations for some endpoints in the significant DVH points (and in their coefficient). However, it is highly likely that the uncertainties due to the change of dose calculation algorithms with time, given their range, should have a minimal impact on the presented models, seeing the large inter-patient variations of absolute DVH values.
Moreover, the analysis of skin dose distributions could be performed in a more efficient way through the use of dosiomics, i.e., the extraction of spatial features of the dose distribution within the breast or in a slab of volume[65]. The advantages of the dosiomics for the skin reactions are: (i) the possibility to consider the volumetric (3D) information of the dose spatial distribution, which is compressed and lose in the DVH (2D representation), thus, weighting the different impacts of the continuous and discontinuous region of high dose within the breast tissue, (ii) the additional information on the geographical location of regions or layers more associated to each specific endpoint, mimicking the voxel-based analysis approach.

Chapter 6

Conclusions

A large mono-institutional population of breast cancer patients was used for developing dosimetric NTCP models for skin reactions following adjuvant radiotherapy. The study endpoints were: (i) any acute grade 2 or plus skin toxicity; (ii) oedema and hyperpigmentation development; (iii) late moderate/severe grade of fibrosis, atrophy, telangectasia and pain; and (iv) liponecrosis. For the first time in these endpoints, the considered Organ at Risk for the dosimetry was the first 5 mm of the breast skin. The PTV volume was confirmed as one of the most impacting factors in the development of any sequela (excepting the liponecrosis). The volume receiving 20 Gy, the 50% of the prescription dose, was applied as a dosimetric descriptor in models for (i), (ii), (iii) and was able to replace PTV giving, in the same time, the possibility to better interpret the damage in terms of irradiated skin as well as being more generalizable, being independent on the contouring phase; in addition, V42 Gy was entered in the model for describing late toxicity (iii). For liponecrosis, the V30 Gy was applied in the dose-response relationship model. Among the treatment and patient factors, lymph node dissection was the most impacting factor for three of the four endpoints (i-ii-iii), and it was included as a covariate in the model together with the dosimetric descriptor. Obesity was identified as a risk factor for early skin reaction, while aromatase inhibitor and hormone therapy and age were found as protective factors in a multivariate model for late toxicity and lipoencrosis, respectively. The cosmetic status after surgery was found to be associated with the development of late fibrosis and was included in that multivariable model to account for the damage to the breast arenchymal tissue caused by the conservative surgery. A differentiated model was developed for the early skin reactions and for oedema and hyperpigmentation to describe the subgroup of patients treated without the bolus application. Two parallel studies are already ongoing to validate the NTCP models on an external population (REQUITE cohort) of European breast cancer patients treated with a similar RT schedule and to test the feasibility of applying the identified dose constraints in the

planning of different RT techniques. At our knowledge, the current study represent the largest series ever published deriving quantitative dose-volume/(surface) effects for breast radiotherapy.

Appendix A

Dosimetric comparison between RT Techniques

The differences in the dose delivery of the RT techniques reflect in the DVHs of the target and organ at risk. Several studies performed multiple comparisons. Here, we reported data from a phantom study on right breast cancer by Liu et al and a second set of in silico studies on breast cancer patients. The phantom study compared the target coverage and dose to the OARs from IMRT, hybrid 3DCRT/IMRT (addition of two medial segments accounting for 30% of the dose), VMAT with non-continuous arc and VMAT with a continuous partial arc. The prescription dose was 50.4 Gy in 28 fractions. VMAT attained the best target coverage with V95$>$ 97.40% and a limited percentage of hotspots with an average V107$<$ 2.05% (especially with VMAT, where it is 0.78%). Conformity Index (CI) and Homogeneity Index (both HI1 and HI2) were also better in the VMAT treatments, with an advantage in the non/continuous modality. This approach also has the benefit of the shortest delivery time, 146 s (against 234s, 245s, and 300s for the cVMAT, Hybrid 3DCRT and IMRT, respectively), reducing the risk of patient motion and discomfort. On the contrary, MU was highest in VMAT (687+-15) and lowest in the hybrid 3DCRT (319+-19), representing the expected effect of a high modulation treatment. Consequences of this characteristic have also impact the dosimetric distribution of the OARs. Details on the dosimetric comparison for PTV and the treatment characteristics are reported in Table 1 and 2.

For the tumor surrounding tissues, hybrid 3DCRT/IMRT has the lowest heart, and contralateral breast mean dose, and continuos VMAT has the lowest mean dose for both the lungs. Therefore, cVMAT has a lower risk of radiation pneumonia, while hybrid 3DCRT should deliver plans with a lower risk of secondary cancer and cardiovascular complications. For the cardiac events, there are reasons to believe that cVMAT could represent a better compromise for the dosimetric characteristic of the heart DVH. First, the average dose to the organ is similar for

the two modalities. Secondly, the maximum dose is lower for cVMAT, which guarantees a more stable mean dose in case of any natural motions. Interestingly the authors also compared the dose in the eye lens and to the skin with non-continuous partial arc representing the best treatment choice, while attention should be paid to the higher scattering dose that contributes to the eye lens when the conventional VMAT is used.

One of the first studies published in literature was by Popescu et al in 2010 on 5 left breast cancer patients. The study compared VMAT with IMRT (9+ coplanar fields) and a modified wide-tangent plan (MWT). Volumes ranged between 334 and 2.170 cc (including chest wall) to cover a large variety of patients. The prescription dose for the PTV was 50 Gy in conventional fractionation. Both VMAT and cIMRT achieved good breast dose homogeneity for all patients considered in this study (all HI > 0.90). For 2 patients, using wedged tangents in the MWT plans resulted in poor breast dose homogeneity (HI< 0.75). These results show that both IMRT techniques produced homogeneous dose distributions. The conformity of the plans was much better with cIMRT and VMAT than with MWT. VMAT plans showed a statistically significant reduction in mean dose to the heart and ipsilateral (left) lung compared with cIMRT.

Jin and colleagues performed an in silico study on 20 left breast cancer patients. Different plans using five different radiation techniques were calculated on each patient, including conventional tangential wedge-based fields (TW); 2) field-in-field (FIF) technique; 3) tangential inverse planning intensity-modulated radiation therapy (T-IMRT); 4) multi-field IMRT (M-IMRT); and 5) volumetric modulated arc therapy (VMAT). The PTV was prescribed to 50 Gy, and the optimization constraint was to ensure 47.5 Gy to 95% of the volume. The coverage was satisfied with all the modalities except the VMAT (94.7%). IMRT (both T-IMRT and 7-IMRT) represented the best options for treatment with good coverage and treatment indices. Regarding the OARs, T-IMRT was again the best RT technique for sparing the organs. Indeed, mean dose, V5, V10, V20, V30 in the ipsilateral lung, heart and coronary artery were always lower than the other techniques. In the lung and the heart, TW showed a lower mean dose than the VMAT with a considerable reduction in the doses receiving doses between 5-10 Gy but longer tail at high doses, represented by more significant percentages at V40. However, this technique is not suggested if we are interested in the spare of coronary artery disease, with TW showing the highest mean dose and V40 with large discrepancy from the other modalities. As reported by the authors, in a non-western population, with small breast volumes, VMAT plan had few advantages in improving the HI of PTV but may decrease the PTV dose coverage and increase the volume irradiates in the lung and contra-lateral breast.

Karpf et al compared 20 left breast cancer treatments in deep inspiration breath

(DIBH) hold with 6 IMRT segments and partial VMAT. IMRT was able to reduce the dose in the contralateral breast, importantly, the heart and the coronary artery while maintaining the same PTV coverage. Regarding the ipsilateral lung, there is a reduction of the volumes within the isodoses < 20 Gy and an increase in the mid-high dose region of the DVH. In general, IMRT significantly reduced V5 to the patient's total body in line with the reduction of the MUs (average discrepancy -156, i.e., 31% of the VMAT MU).

Chen et al. studied a mixed population of 30 patients. Treatment modalities were 7, including a tangential VMAT with 50° extension on each side. Techniques with tangential field arrangement resulted in better OARs dosimetry than those with multi-fields and arcs arrangements. Attallah obtained similar results on 19 left breast patients. They concluded that the 3CDRT provided a lower dose to the contralateral organs (breast and lung), especially, in case of large breast volumes, with no nodal irradiation and when a boost is given. According to the reported studies, definining the best treatment technique for the breast district is not possible. The first reason is that plan objectives can vary on the patient history and characteristics; secondly, in a retrospective planning study, the dosimetric data obtained might be different from actually delivered doses to patients in real-life clinical situations. PTV coverage is influenced by the patient geometry and target volume with 3DCRT representing the best option for low-mid size breast. IMRT can be suggested in case of patients with unfavourable geometry or dysfunction in the lung or in the heart. VMAT can help for plan homogeneity and in reducing the DVH tail in the OARs.

Table 2. Comparison of PTV dose-volume histogram (DVH) parameters in 4 different treatment plans.

Structures	Continuous Partial Arc	Non-Continuous Partial Arc	Hybrid 3D-CRT/IMRT	IMRT
Mean dose (Gy)	52.05 ± 0.09	51.61 ± 1.33	51.82 ± 1.52	51.81 ± 1.45
Maximum dose (Gy)	55.88 ± 0.16	55.07 ± 0.08	56.15 ± 0.07	55.52 ± 0.08
minimal dose (Gy)	25.60 ± 0.16	23.69 ± 1.23	21.67 ± 0.15	23.00 ± 0.04
V100 (%)	97.42 ± 0.09	92.39 ± 0.23	87.61 ± 1.23	89.12 ± 1.43

Table 2. *Cont.*

Structures	Continuous Partial Arc	Non-Continuous Partial Arc	Hybrid 3D-CRT/IMRT	IMRT
V95 (%)	97.42 ± 0.07	97.41 ± 0.9	95.77 ± 1.18	96.62 ± 2.01
V105 (%)	18.59 ± 0.14	18.81 ± 0.11	15.31 ± 1.01	14.39 ± 1.54
V107 (%)	2.05 ± 0.06	0.78 ± 0.04	2.44 ± 0.10	2.38 ± 0.07
V110 (%)	0.10 ± 0.11	0.00 ± 0.00	0.02 ± 0.01	0.01 ± 0.01
D2 (Gy)	53.93 ± 1.45	53.60 ± 2.73	54.25 ± 1.61	54.25 ± 1.48
D98 (Gy)	47.21 ± 0.98	47.15 ± 1.44	45.67 ± 1.77	46.4 ± 1.22
CI	0.74 ± 0.01	0.74 ± 0.01	0.68 ± 0.03	0.64 ± 0.05
HI_1	0.79 ± 0.02	0.89 ± 0.11	0.71 ± 0.21	0.78 ± 0.11
HI_2	13.33 ± 0.01	12.79 ± 0.03	17.02 ± 0.03	15.57 ± 0.04

Vx (%): x % of the prescribed dose volume; Dx (Gy): a volume received greater than x Gy; CI: conformity index; HI: Homogeneity Index.

Table 3. Comparison of normal tissue DVH parameters in four different treatment plans.

Structures	Continuous Partial Arc	Non-Continuous Partial Arc	Hybrid 3D-CRT/IMRT	IMRT
Heart				
Mean dose (Gy)	1.73 ± 0.07	3.15 ± 0.03	1.47 ± 0.02	4.35 ± 0.01
minimal dose (Gy)	0.71 ± 0.04	1.04 ± 0.04	0.30 ± 0.01	1.93 ± 0.03
Maximum dose (Gy)	5.82 ± 0.02	1.47 ± 0.07	9.52 ± 0.08	12.38 ± 0.06
V5Gy (%)	0.07 ± 0.01	0.12 ± 0.01	0.07 ± 0.01	0.27 ± 0.03
V10Gy (%)	0.00 ± 0.00	0.70 ± 0.03	0.00 ± 0.00	0.005 ± 0.01
V50.40Gy (%)	0.00 ± 0.00	0.00 ± 0.00	0.00 ± 0.00	0.00 ± 0.00
Right lung (ipsilateral)				
Mean dose (Gy)	8.32 ± 1.61	10.71 ± 0.09	10.14 ± 1.47	12.76 ± 1.23
minimal dose (Gy)	0.80 ± 0.04	0.50 ± 0.03	0.27 ± 0.01	1.65 ± 0.01
Maximum dose (Gy)	54.06 ± 1.08	52.32 ± 0.06	51.88 ± 0.09	52.37 ± 0.05
V5Gy (%)	32.56 ± 0.91	39.69 ± 0.02	45.12 ± 0.77	60.82 ± 0.32
V10Gy (%)	20.02 ± 0.13	8.96 ± 0.10	30.97 ± 0.58	35.80 ± 0.18
V20Gy (%)	12.96 ± 0.34	20.43 ± 1.00	17.55 ± 1.69	23.33 ± 1.91
V30Gy (%)	9.16 ± 0.45	14.30 ± 0.09	12.09 ± 1.01	17.54 ± 0.09
V40Gy (%)	5.80 ± 0.69	8.38 ± 0.45	7.69 ± 0.33	11.60 ± 0.17
V50.40Gy (%)	1.01 ± 0.09	0.24 ± 0.01	0.19 ± 0.04	0.79 ± 0.01

Table 1. Plan comparison parameters, mean values and range for VMAT, cIMRT and MWT techniques treating the left breast/chest wall and regional nodes including IMNs for the five patients considered in this study

Structure	Parameters	VMAT Plan	cIMRT Plan	MWT Plan
Left breast/chest wall, PTV50	V47.5 (%)	96.9 (95.5 - 98.5)	97.7 (95.7–99.4)	92.0 (83.7–97.8)
	$D_{2\%}$ (Gy)	51.8 (51.2 - 52.1)	52.5 (51.8–53.0)	54.3 (52.2 -58.5)
Regional Nodes, PTV45	V42.75 (%)	99.4 (99.0–99.8)	99.6 (99.3–99.8)	95.3 (91.3–100)
	$D_{2\%}$ (Gy)	49.1 (48.8 - 49.6)	49.1 (48.7 - 49.5)	53.9 (52.8- 54.8)
Heart	Mean (Gy)	10.9 (9.2 - 11.0)*	14.1 (13.1–14.7)	10.6 (8.4–13.4)
	V45 (%)	0.3 (0.05 -0.99)**	0.1 (0.03–0.14)	6.8 (2.3–9.3)
	V30 (%)	2.6 (1.7–3.3)**	3.5 (2.6–4.6)	16.4 (12.2–23.4)
	V10 (%)	35.7 (28.7 - 42.5)*	69.6 (58.4–76.2)	24.1 (18.1 -33.6)
	V5 (%)	83.0 (75.0 - 89.9)*	100.0 (99.95 - 100)	31.9 (25.7–42.1)
Ipsilateral (Left) Lung	Mean (Gy)	11.6 (11.2 -12.3)*	13.1 (12.8 - 13.5)	18.1 (14.2 -22.3)
	V20 (%)	16.9 (15.8 - 18.4)**	17.3 (16.1 - 18.6)	37.3 (28.8–48.6)
	V10 (%)	40.3 (37.7 - 43.5)*	52.4 (46.2 - 57.4)	41.1 (33.1–52.0)
	V5 (%)	70.2 (65.1 -74.9)*	91.9 (85.7 - 99.8)	46.8 (39.3–56.5)
Contralateral (Right) Lung	Mean (Gy)	2.9 (2.6–3.4)*	5.5 (5.0 - 6.0)	0.8 (0.6 -1.1)
	V5 (%)	8.1 (3.2–14.8)*	51.3 (40.8 -62.2)	0.4 (0.0–1.6)
Contralateral (Right) Breast	Mean (Gy)	3.2 (2.5 - 4.0)*	4.3 (3.8–4.7)	4.4 (1.3–12.5)
	V5 (cc)	52.3 (6.3–136.1)	130.9 (30.6–371.3)	85.2 (5.1–369.0)
Healthy Tissue	Mean (Gy)	7.1 (6.5 - 7.5)*	8.4 (7.9 - 9.2)	7.4 (5.7–9.6)
	V5 (cc)	7059 (4748–10534)*	9606 (6766–12912)	4381 (2259–7928)

Abbreviations: Vn(%) = percent volume receiving nGy or grater; $D_{2\%}$ = dose to 2% of the volume.
* p value <0.05 cf cIMRT.
** p value <0.05 cf MWT.

Table 2 The PTV dose parameters of five plans ($\bar{x} \pm d$)

Parameters	TW	FIF	T-IMRT	7-IMRT	VMAT
D98(Gy)	47.3±0.4	47.0±0.4	47.0±0.6	47.3±0.6	46.4±0.6
D2(Gy)	53.2±0.6	52.0±0.6	52.7±0.6	52.4±0.5	53.4±0.7
D50(Gy)	50.6±0.6	50.7±0.4	50.7±0.4	50.4±0.4	51.0±0.4
V95%	96.2 ± 1.6^{A}	95.6 ± 1.6^{A}	96.8 ± 1.7^{A}	96.1 ± 1.7^{A}	94.7 ± 1.2^{A}
CI	2.0 ± 0.5^{Aa}	1.7 ± 0.4^{A}	1.6 ± 0.3^{Ab}	1.3 ± 0.1^{Bb}	1.4 ± 0.2^{Bb}
HI	0.13 ± 0.02^{A}	0.11 ± 0.02^{B}	0.11 ± 0.03^{B}	0.11 ± 0.02^{B}	0.14 ± 0.02^{A}

A had significant difference with B ($p<0.05$), and, a had significant difference with b ($p<0.05$). Otherwise the difference was not significant between any two ($p>0.05$).

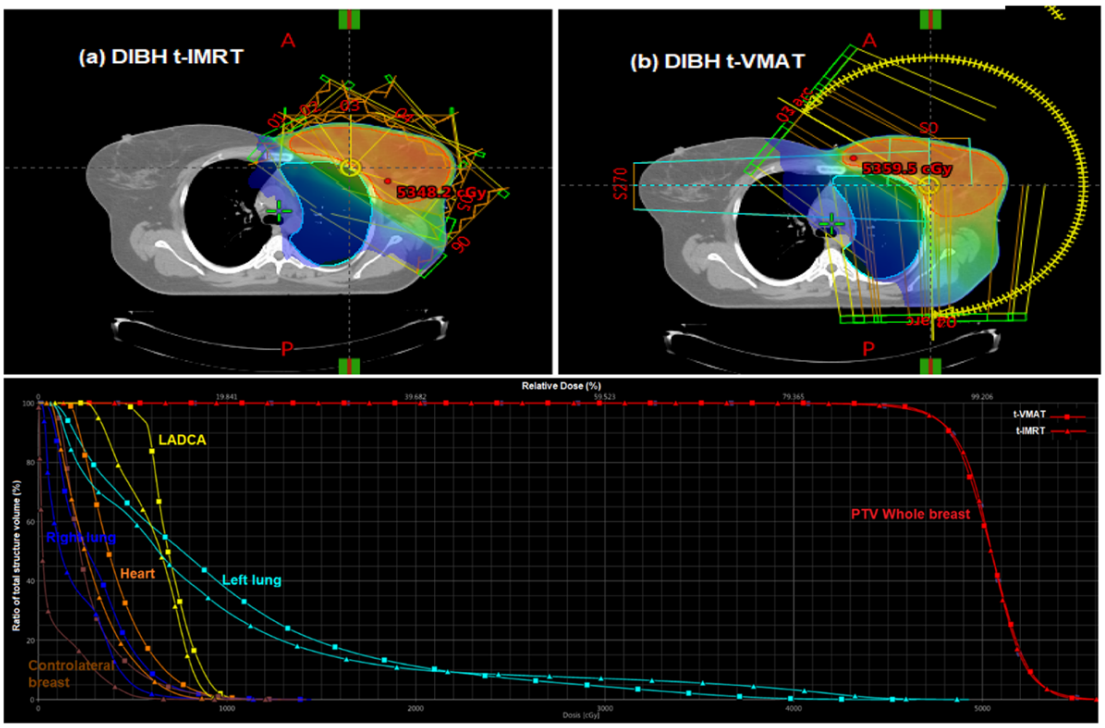

Fig. 1 Beam arrangement, isodose distribution and DVH of target volume and organs at risk in both **a** DIBH t-IMRT and **b** DIBH t-VMAT plans for a left-sided breast cancer case

Table 4. Dosimetric parameter outcomes for PTV and OARs, along with required planning times required between the various techniques

Parameter	3DCRT	3DFIF	IMRT MF5	tIMRT	tVMAT	Ecomp	Hybrid
PTV_{Dmax} (Gy)	46.01 ± 1.52	45.07 ± 0.36	46.38 ± 0.53	45.03 ± 0.69	46.35 ± 0.70	44.61 ± 0.71	44.87 ± 0.59
$PTV_{V95\%}$ (%)	98.19 ± 2.80	97.97 ± 3.02	99.05 ± 1.32	98.79 ± 2.01	95.73 ± 4.24	98.24 ± 2.69	98.59 ± 2.38
Conformity Index	0.98 ± 0.03	0.98 ± 0.03	0.99 ± 0.01	0.99 ± 0.02	0.96 ± 0.04	0.98 ± 0.03	0.98 ± 0.03
Homogeneity Index	1.09 ± 0.03	1.08 ± 0.03	1.10 ± 0.01	1.06 ± 0.03	1.11 ± 0.03	1.06 ± 0.03	1.07 ± 0.03
IL_{Dmean} (Gy)	4.81 ± 2.48	4.70 ± 2.37	8.21 ± 1.01	4.86 ± 1.96	8.97 ± 2.24	5.18 ± 2.56	5.36 ± 2.38
IL_{V5Gy} (%)	15.44 ± 7.84	15.61 ± 7.88	57.62 ± 9.20	16.84 ± 7.34	43.51 ± 9.87	17.50 ± 8.74	18.07 ± 8.35
IL_{V20Gy} (%)	8.61 ± 5.69	8.58 ± 5.64	9.13 ± 3.79	9.23 ± 5.24	16.68 ± 5.64	9.94 ± 6.57	10.44 ± 6.51
IL_{V30Gy} (%)	7.18 ± 5.24	7.06 ± 5.13	2.77 ± 2.09	6.44 ± 3.88	9.65 ± 4.50	7.37 ± 5.83	7.92 ± 5.05
CL_{Dmean} (Gy)	0.04 ± 0.03	0.04 ± 0.03	4.00 ± 1.56	0.04 ± 0.03	0.47 ± 0.32	0.05 ± 0.03	0.06 ± 0.03
CL_{V10Gy} (%)	0 ± 0	0 ± 0	10.38 ± 6.84	0 ± 0	0.23 ± 0.55	0 ± 0	0 ± 0
CB_{Dmax} (Gy)	8.02 ± 12.74	7.87 ± 12.03	22.00 ± 11.46	7.25 ± 11.47	27.61 ± 7.39	8.20 ± 12.64	9.29 ± 13.34
CB_{Dmean} (Gy)	0.16 ± 0.12	0.17 ± 0.12	2.49 ± 1.83	0.14 ± 0.13	2.30 ± 2.08	0.18 ± 0.15	0.30 ± 0.53
CB_{V5Gy} (%)	0.12 ± 0.39	0.16 ± 0.53	14.52 ± 17.11	0.13 ± 0.43	14.86 ± 15.68	0.17 ± 0.50	0.18 ± 0.51
$Heart_{Dmean}$ (Gy)	1.52 ± 1.14	1.51 ± 1.11	4.20 ± 0.66	1.80 ± 0.74	4.98 ± 1.63	1.91 ± 0.96	2.15 ± 1.03
$Heart_{V5Gy}$ (%)	2.97 ± 3.48	2.79 ± 3.11	23.90 ± 6.62	4.28 ± 3.03	25.28 ± 8.24	4.63 ± 3.76	5.00 ± 3.96
$Heart_{V20Gy}$ (%)	1.45 ± 2.26	1.45 ± 2.26	1.12 ± 2.07	1.99 ± 1.95	6.80 ± 4.19	2.58 ± 2.52	2.89 ± 2.77
$Liver_{Dmean}$ (Gy)	1.22 ± 1.78	1.20 ± 1.72	6.56 ± 4.02	1.48 ± 1.30	4.23 ± 3.05	1.69 ± 1.61	1.82 ± 1.48
$Liver_{V10Gy}$ (%)	1.73 ± 4.19	1.76 ± 4.21	27.00 ± 20.02	3.00 ± 3.54	12.89 ± 10.27	3.27 ± 3.91	3.55 ± 3.94
$Body_{V10Gy}$ (%)	8.07 ± 2.08	8.12 ± 2.10	16.71 ± 3.65	8.84 ± 1.82	13.40 ± 2.71	9.13 ± 1.97	9.29 ± 1.97
Total MUs	311 ± 21	303 ± 15	142 ± 19	500 ± 78	364 ± 49	520 ± 42	465 ± 53
Planning time (min)	14 ± 2	16 ± 3	80 ± 14	16 ± 2	39 ±2	15 ± 3	18 ± 2

Values are presented as mean ± standard deviation.
PTV, planning target volume; OAR, organs-at-risk; 3DCRT, three-dimensional conformal radiation therapy; 3DFIF, three-dimensional field-in-field; IMRT MF5, 5-field intensity-modulated radiotherapy; tIMRT, tangential IMRT; tVMAT, tangential volumetric modulated arc therapy; Ecomp, electronic tissue compensation; IL, ipsilateral lung; CL, contralateral lung; CB, contralateral breast; MUs, monitor units.

Appendix B

Dosimetric Dose Calculation Algorithm

The PBC algorithm is a Pencil Beam Convolution algorithm in which the pencil kernels are derived from measured data, as explained in the formalism presented by Storchi et al. Instead, the AAA is a Pencil Beam Convolution/superposition algorithm. The configuration model is based on pre-calculated Monte Carlo-determined basic physical parameters adapted to the measured clinical beam data introduced in the system by the user. These parameters are then used to determine the characteristics of the fluence and energy of both photons and electrons in the beam. They are then used to assess their scattering properties in water-equivalent media. Differently from the PBC, the clinical beam in AAA is represented by a multiple source model divided into a primary photon source (the photons coming directly from the target), scattered extra-focal photons and the contaminating electrons. The electron contamination source, which is important in calculating the build-up region, is modelled by the AAA with a depth-dependent curve, approximated by two Gaussians and an energy deposition function, defined by parameters optimized to reproduce the field size dependence. The Acuros XB is based on applying the LBTE that describes the interactions of radiation particles with matter. This is based on approximate numerical methods. Monte Carlo (MC) and explicit LBTE solvers, as Acuros XB, should converge to the same final results. In practice, both methods are affected by potential inaccuracies depending on the sampling level of probability distribution functions applied during MC simulations or the application of variables discretization during explicit LBTE solution. A characteristic of LBTE solvers, compared to MC simulations, is the absence of uncertainties due to statistical noise in the calculated dose. Acuros XB implementation consists of two main components: i) the photon beam source model and ii) the radiation transport model.

Appendix C

Toxicity Models

NTCP Model for ACUG2 (Whole population - Clinical Model)
AUC = 0.61, calib = 0.00 + 1.03 x, HL p = 0.29

Variable	Coeff.	Std. Err.	P>—z—	OR
ALND	0.447994	0.199344	0.024619	1.565169
Bolus	0.469055	0.201017	0.019626	1.598483
PTV Volume	0.001122	0.000224	5.38E-07	1.001122
Constant	-2.76632	0.21506	0	0.062893

NTCP Model for ACUG2 (Whole population - Dosimetric Model)
AUC = 0.61 calib = 0.00 + 1.02 x, HL p = 0.85

Variable	Coeff.	Std. Err.	P>—z—	OR
ALND	0.419	0.199	0.036	1.52
obesity	0.598	0.199	0.003	1.818
V20Gy	0.004	0.002	0.039	1.004
Constant	-2.926	0.448	0	0.054

NTCP Model for ACUG2 (Pts without Bolus - Clinical Model)
AUC = 0.64 calib = 0.00 + 1.01 x, HL p = 0.91

Variable	Coeff.	Std. Err.	P>—z—	OR
ALND	0.453296	0.230504	0.049235	1.57349
PTV Volume	0.001128	0.000264	1.97E-05	1.001128
hypertension	0.384236	0.200876	0.055773	1.468492
Constant	-2.93108	0.250415	0	0.053339

NTCP Model for ACUG2 (Pts without Bolus - Dosimetric Model 1)
AUC = 0.64 calib = 0.00 + 1.01 x, HL p = 0.91

Variable	Coefficient	Std. Error	P	OR
ALND	0.45798	0.22922	0.0457	1.580877385
V200	0.0082229	0.0023657	0.0005	1.008256801
hypertension	0.43081	0.19892	0.0303	1.538503207
Constant	-3.84518	0.53213	<0.0001	0.021382552

NTCP Model for ACUG2 (Pts without Bolus - Dosimetric Model 2)
AUC = 0.64, calib = 0.00 + 0.99 x, HL p = 0.36

Variable	Coefficient	Std. Error	P	OR
ALND	0.4246	0.23039	0.0653	1.528978706
V200	0.006163	0.0025525	0.0158	1.00618203
obesity	0.61504	0.22132	0.0055	1.849730587
Constant	-3.41502	0.55028	<0.0001	0.032875749

NTCP Model for ACUG2 (Pts without Bolus - Dosimetric Model 3)
AUC = 0.64, calib = 0.00 + 0.99 x, HL p = 0.57

Variable	Coefficient	Std. Error	P	OR
hypertension	0.3726	0.20073	0.0634	1.451503622
V200	0.0056983	0.0025501	0.0254	1.005714566
obesity	0.58705	0.2216	0.0081	1.798674491
Constant	-3.36459	0.5462	<0.0001	0.034576189

NTCP Model for ACUG2 (Pts with Bolus - Dosimetric Model 3)
AUC = 0,65, calib = 0.00 + 0.99 x, HL p = 0.47

Variable	Coefficient	Std. Error	P	OR
PTV Volume	0.0011168	0.00046782	0.017	1.001117424
age	-0.04013	0.014645	0.0061	0.960664545
Constant	0.14455	0.83147	0.862	1.155519469

NTCP Model for EH (Clinical Model - Whole Population)
AUC = 0.75, calib = 0.01 + 0.89 x, HL p = 0.64

Variable	Coefficient	Std.˜Error	P	OR
PTV Volume	0.0017796	0.0003274	<0.0001	0.998221983
ALND	1.12898	0.30142	0.0002	0.323362918
Constant	-4.78731	0.35922	<0.0001	

NTCP Model for EH (Dosimetric Model - Whole Population)
AUC = 0.74, calib = 0.01 + 0.87 x, HL p = 0.54

Variable	Coefficient	Std.˜Error	P	OR
V20 Gy	0.014686	0.0030704	<0.0001	0.985421313
ALND	1.13591	0.29939	0.0001	0.32112976
Constant	-6.59118	0.74351	<0.0001	

NTCP Model for EH (ClinicalModel - Population without bolus)
AUC = 0.76, calib = 0.00 + 0.92 x, HL p = 0.54

Variable	Coefficient	Std.˜Error	P	OR
PTV Volume	0.0019026	0.00036834	<0.0001	0.998099209
ALND	1.23125	0.32266	0.0001	0.29192744
Constant	-4.86149	0.41567	<0.0001	

NTCP Model for EH (ClinicalModel - Population without bolus)
AUC = 0.75, calib = 0.00 + 0.93 x, HL p = 0.33

Variable	Coefficient	Std.˜Error	P	OR
V20 Gy	0.016459	0.0035424	<0.0001	0.983675709
ALND	1.23039	0.32038	0.0001	0.292178606
Constant	-6.9351	0.87096	<0.0001	

NTCP Model for FATP (Clinical Model - Whole Population)
AUC = 0.82, calib = 0.00 + 0.96 x, HL p = 0.09

Variable	Coeff.	Std. Err.	P>—z—	OR
ALND	0.775053021	0.379292438	0.04101107	2.170707216
Aromatase Inhibitor	-0.855697007	0.350730146	0.014697066	0.424986869
TargettargetNEW	0.002209254	3.87E-04	1.13E-08	1.002211696
Cosmesis	2.109468164	0.393385456	8.21E-08	8.243855741
Constant	-5.22543146	0.46350308	0	0.005378039

NTCP Model for FATP (Dosimetric Model - Whole Population)
AUC = 0.78, calib = 0.00 + 0.1.02 x, HL p = 0.081

Variable	Coeff.	Std. Err.	P>—z—	OR
ALND	0.818614	0.375733	0.029353	2.267355
AROMATASE INHIBITOR	-0.77891	0.348272	0.02532	0.458907
Cosmesis	1.951327	0.3846	3.90E-07	7.038024
V20 Gy	0.015864	0.003478	5.10E-06	1.01599
V42 Gy	0.08636	0.044511	0.052355	1.090199
Constant	-7.00446	0.866005	0	0.000908

Appendix D

Supporting the discussion

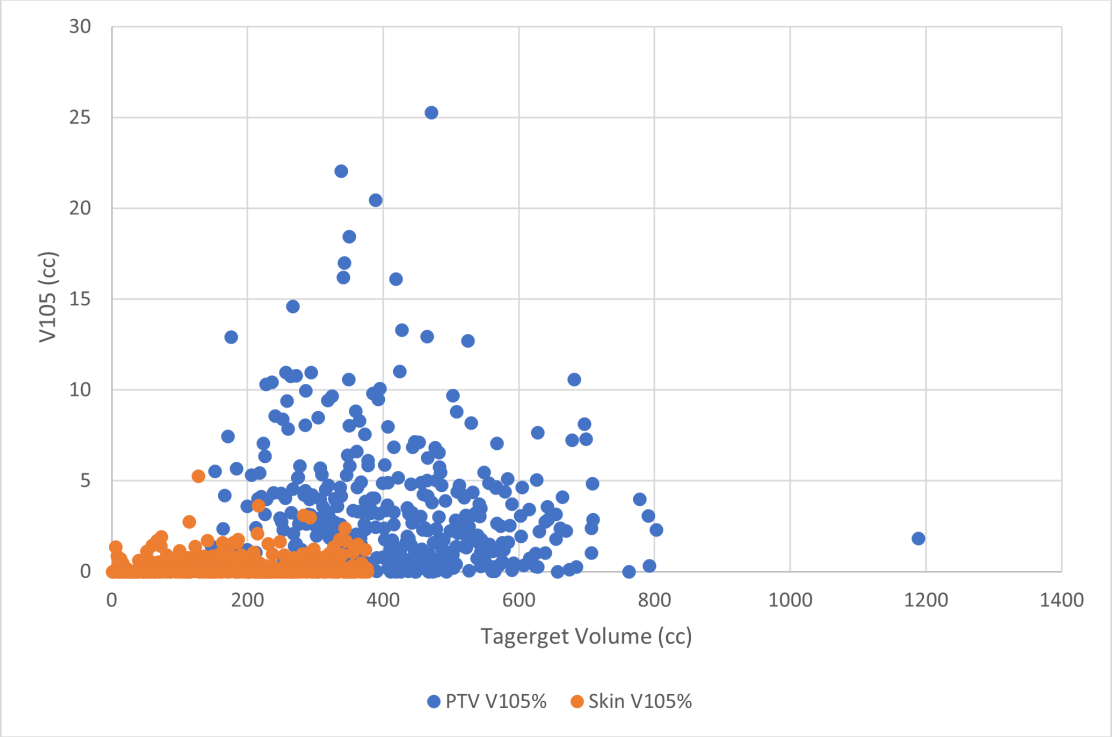

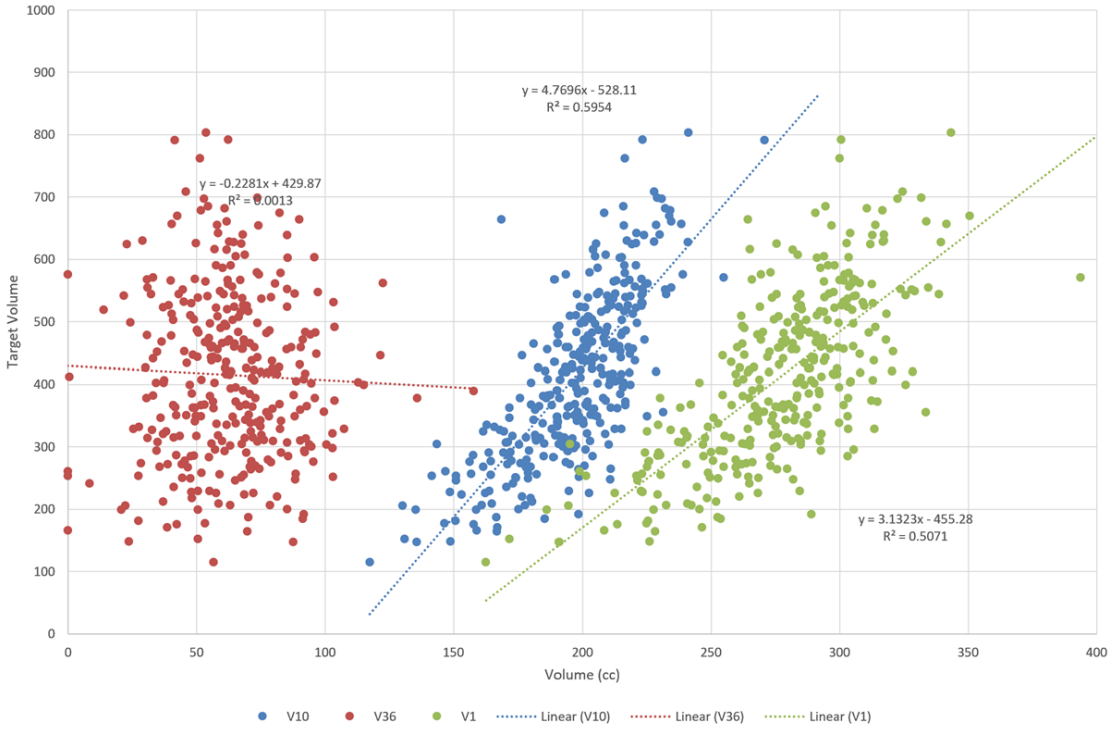
y = 4.7696x - 528.11
R² = 0.5954
y = -0.2281x + 429.87
R² = 0.0013
y = 3.1323x - 455.28
R² = 0.5071
Target Volume
Volume (cc)
V10
V36
V1
Linear (V10)
Linear (V36)
Linear (V1)

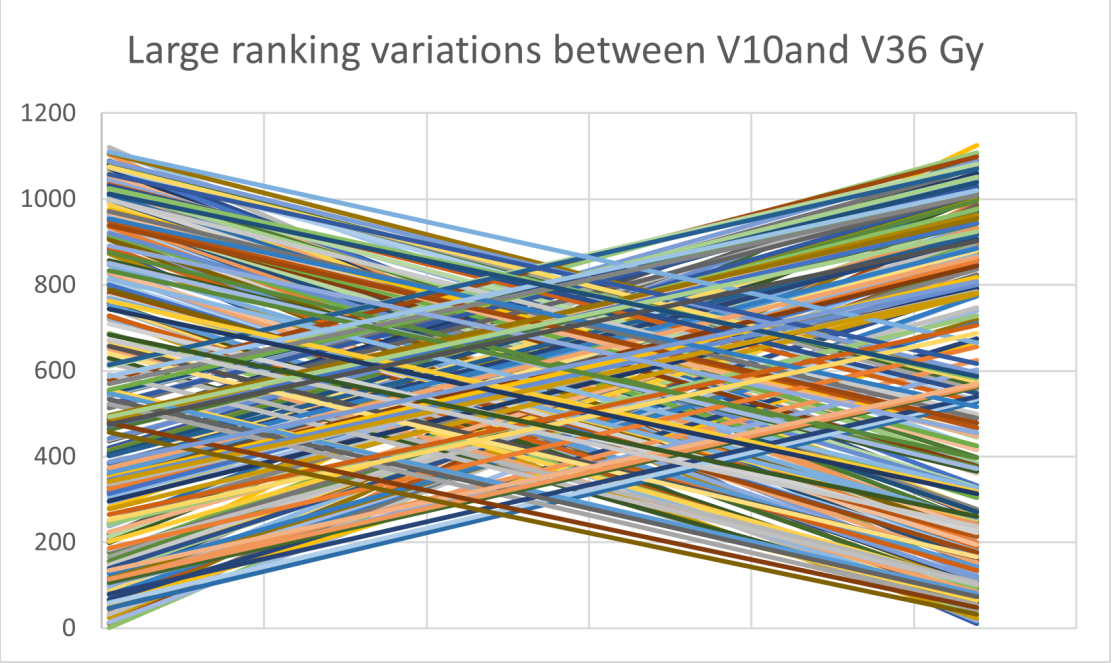
Large ranking variations between V10and V36 Gy

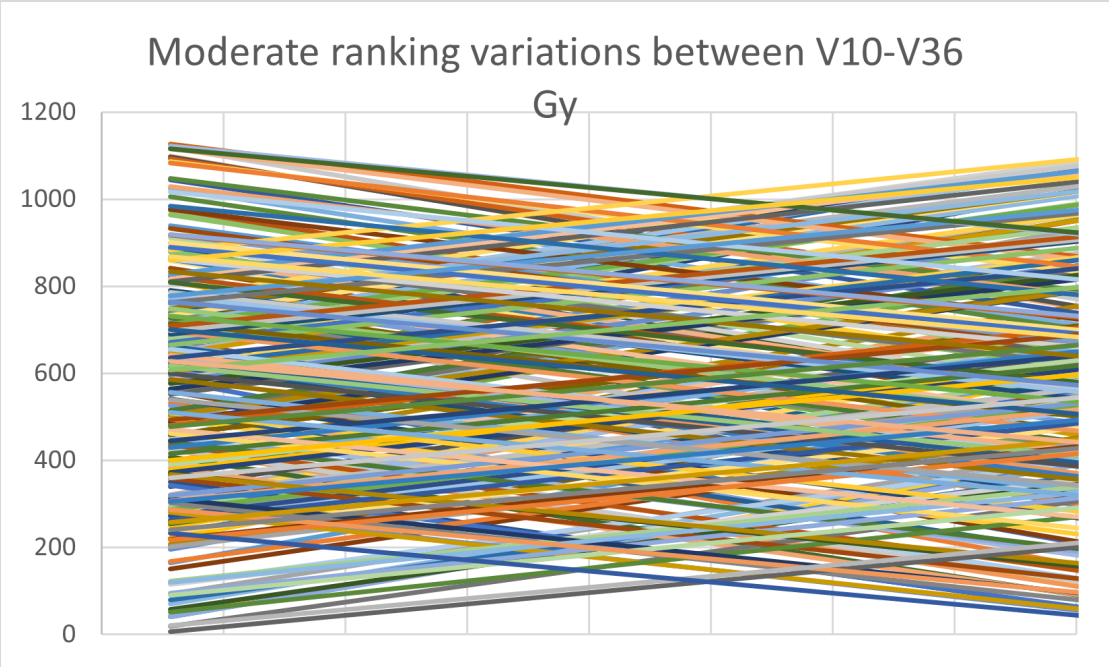

	ACUG2	**p-value**	**EH**	**p-value**	**FATP**	**p-value**	**Liponecrosis**	**p-value**
Vol I-II (<642 cc)	11.1	**0.003**	2.3	**<0.0001**	2.2	**<0.0001**	7.6	0.008
Vol II-III (642-913 cc)	18.2		3.5		3		11.6	
Vol III-IV (>913 cc)	20		10.9		7.9		15.2	
ALND no	13.8	**0.01**	3.4	**<0.0001**	3.1	0.07	10.9	0.34
ALND yes	20.6		10.1		5.9		8.6	
HotSpot I-II-III Q	15.1	0.99	4.2	**0.04**	3	0.06	11.8	**0.02**
HotsSpot IV Q	15.1		6.1		5.7		6.7	
V20 I-II-III Q	13.7	**<0.0001**	2.7	**<0.0001**	2.4	**<0.0001**	9.1	**0.01**
V20 IV Q	19.1		10.4		7.9		14.5	

Bibliography

[1] R. Abdlaty, L. Doerwald-Munoz, A. Madooei, S. Sahli, S.-C. A. Yeh, J. Zerubia, R. K. Wong, J. E. Hayward, T. J. Farrell, and Q. Fang. Hyperspectral imaging and classification for grading skin erythema. *Frontiers in Physics*, 6:72, 2018.

[2] M. Alexander, W. Brooks, and S. Blake. Normal tissue complication probability modelling of tissue fibrosis following breast radiotherapy. *Physics in Medicine & Biology*, 52(7):1831, 2007.

[3] S. S. Almberg, T. Lindmo, and J. Frengen. Superficial doses in breast cancer radiotherapy using conventional and imrt techniques: a film-based phantom study. *Radiotherapy and Oncology*, 100(2):259–264, 2011.

[4] J. O. Archambeau, R. Pezner, and T. Wasserman. Pathophysiology of irradiated skin and breast. *International Journal of Radiation Oncology* Biology* Physics*, 31(5):1171–1185, 1995.

[5] M. Avanzo, G. Pirrone, M. Mileto, S. Massarut, J. Stancanello, M. Baradaran-Ghahfarokhi, A. Rink, L. Barresi, L. Vinante, E. Piccoli, et al. Prediction of skin dose in low-kv intraoperative radiotherapy using machine learning models trained on results of in vivo dosimetry. *Medical physics*, 46(3):1447–1454, 2019.

[6] M. Avanzo, J. Stancanello, M. Trovò, R. Jena, M. Roncadin, M. G. Trovò, and E. Capra. Complication probability model for subcutaneous fibrosis based on published data of partial and whole breast irradiation. *Physica Medica*, 28(4):296–306, 2012.

[7] M. Back, M. Guerrieri, C. Wratten, and A. Steigler. Impact of radiation therapy on acute toxicity in breast conservation therapy for early breast cancer. *Clinical Oncology*, 16(1):12–16, 2004.

[8] G. C. Barnett, C. M. West, C. E. Coles, P. D. Pharoah, C. J. Talbot, R. M. Elliott, G. A. Tanteles, R. P. Symonds, J. S. Wilkinson, A. M. Dunning,

et al. Standardized total average toxicity score: a scale-and grade-independent measure of late radiotherapy toxicity to facilitate pooling of data from different studies. *International Journal of Radiation Oncology* Biology* Physics*, 82(3):1065–1074, 2012.

[9] H. Bartelink, P. Maingon, P. Poortmans, C. Weltens, A. Fourquet, J. Jager, D. Schinagl, B. Oei, C. Rodenhuis, J.-C. Horiot, et al. Whole-breast irradiation with or without a boost for patients treated with breast-conserving surgery for early breast cancer: 20-year follow-up of a randomised phase 3 trial. *The lancet oncology*, 16(1):47–56, 2015.

[10] B. M. Beadle, W. A. Woodward, S. L. Tucker, E. D. Outlaw, P. K. Allen, J. L. Oh, E. A. Strom, G. H. Perkins, W. Tereffe, T.-K. Yu, et al. Ten-year recurrence rates in young women with breast cancer by locoregional treatment approach. *International Journal of Radiation Oncology* Biology* Physics*, 73(3):734–744, 2009.

[11] S. M. Bentzen, H. D. Thames, and M. Overgaard. Latent-time estimation for late cutaneous and subcutaneous radiation reactions in a single-follow-up clinical study. *Radiotherapy and Oncology*, 15(3):267–274, 1989.

[12] C. Bergom, A. Currey, N. Desai, A. Tai, and J. B. Strauss. Deep inspiration breath hold: techniques and advantages for cardiac sparing during breast cancer irradiation. *Frontiers in oncology*, 8:87, 2018.

[13] J. D. Boice Jr, E. B. Harvey, M. Blettner, M. Stovall, and J. T. Flannery. Cancer in the contralateral breast after radiotherapy for breast cancer. *New England Journal of Medicine*, 326(12):781–785, 1992.

[14] F. N. Bray, B. J. Simmons, A. H. Wolfson, and K. Nouri. Acute and chronic cutaneous reactions to ionizing radiation therapy. *Dermatology and therapy*, 6(2):185–206, 2016.

[15] F. N. Bray, B. J. Simmons, A. H. Wolfson, and K. Nouri. Acute and chronic cutaneous reactions to ionizing radiation therapy. *Dermatology and therapy*, 6(2):185–206, 2016.

[16] J. Brierley, I. Paterson, R. Lallemand, and A. Rostom. The influence of breast size on late radiation reaction following excision and radiotherapy for early breast cancer. *Clinical Oncology*, 3(1):6–9, 1991.

[17] A. M. Brunt, J. S. Haviland, D. A. Wheatley, M. A. Sydenham, A. Alhasso, D. J. Bloomfield, C. Chan, M. Churn, S. Cleator, C. E. Coles, et al. Hypofractionated breast radiotherapy for 1 week versus 3 weeks (fast-forward):

5-year efficacy and late normal tissue effects results from a multicentre, non-inferiority, randomised, phase 3 trial. *The Lancet*, 395(10237):1613–1626, 2020.

[18] N. Burnet, G. Barnett, R. Elliott, D. Dearnaley, P. Pharoah, A. Dunning, and C. West. Rapper: the radiogenomics of radiation toxicity. *Clinical Oncology*, 25(7):431–434, 2013.

[19] Y. Cao, X. Yang, Z. Yang, X. Qiu, Z. Lv, M. Lei, G. Liu, Z. Zhang, and Y. Hu. Superficial dose evaluation of four dose calculation algorithms. *Radiation Physics and Chemistry*, 137:23–28, 2017.

[20] P. Ciammella, A. Podgornii, M. Galeandro, R. Micera, D. Ramundo, T. Palmieri, E. Cagni, and C. Iotti. Toxicity and cosmetic outcome of hypofractionated whole-breast radiotherapy: predictive clinical and dosimetric factors. *Radiation oncology*, 9(1):1–10, 2014.

[21] A. Cicchetti, F. Laurino, L. Possenti, T. Rancati, and P. Zunino. In silico model of the early effects of radiation therapy on the microcirculation and the surrounding tissues. *Physica Medica*, 73:125–134, 2020.

[22] C. E. Coles, C. L. Griffin, A. M. Kirby, J. Titley, R. K. Agrawal, A. Alhasso, I. S. Bhattacharya, A. M. Brunt, L. Ciurlionis, C. Chan, et al. Partial-breast radiotherapy after breast conservation surgery for patients with early breast cancer (uk import low trial): 5-year results from a multicentre, randomised, controlled, phase 3, non-inferiority trial. *The Lancet*, 390(10099):1048–1060, 2017.

[23] S. Collette, L. Collette, T. Budiharto, J.-C. Horiot, P. M. Poortmans, H. Struikmans, W. Van den Bogaert, A. Fourquet, J. J. Jager, W. Hoogenraad, et al. Predictors of the risk of fibrosis at 10 years after breast conserving therapy for early breast cancer–a study based on the eortc trial 22881–10882 'boost versus no boost'. *European Journal of Cancer*, 44(17):2587–2599, 2008.

[24] D. Curran, J. Van Dongen, N. K. Aaronson, G. Kiebert, I. Fentiman, F. Mignolet, and H. Bartelink. Quality of life of early-stage breast cancer patients treated with radical mastectomy or breast-conserving procedures: results of eortc trial 10801. *European Journal of Cancer*, 34(3):307–314, 1998.

[25] S. C. Darby, M. Ewertz, P. McGale, A. M. Bennet, U. Blom-Goldman, D. Brønnum, C. Correa, D. Cutter, G. Gagliardi, B. Gigante, et al. Risk of ischemic heart disease in women after radiotherapy for breast cancer. *New England Journal of Medicine*, 368(11):987–998, 2013.

[26] F. De Rose, D. Franceschini, G. Reggiori, A. Stravato, P. Navarria, A. Ascolese, S. Tomatis, P. Mancosu, and M. Scorsetti. Organs at risk in lung sbrt. *Physica Medica*, 44:131–138, 2017.

[27] M. De Santis, F. Bonfantini, F. Di Salvo, M. Dispinzieri, E. Mantero, F. Soncini, P. Baili, M. Sant, G. Bianchi, C. Maggi, et al. Factors influencing acute and late toxicity in the era of adjuvant hypofractionated breast radiotherapy. *The Breast*, 29:90–95, 2016.

[28] S. Delanian, R. Porcher, S. Balla-Mekias, and J.-L. Lefaix. Randomized, placebo-controlled trial of combined pentoxifylline and tocopherol for regression of superficial radiation-induced fibrosis. *Journal of Clinical Oncology*, 21(13):2545–2550, 2003.

[29] J. W. Denham and M. Hauer-Jensen. The radiotherapeutic injury–a complex 'wound'. *Radiotherapy and Oncology*, 63(2):129–145, 2002.

[30] J. Dong, Y. Yang, D. Han, Q. Zhao, C. Liu, H. Sun, Z. Wang, H. Lin, and W. Huang. Hypofractionated simultaneous integrated boost radiotherapy versus conventional fractionation radiotherapy of early breast cancer after breast-conserving surgery: Clinical observation and analysis. *Technology in Cancer Research & Treatment*, 20:15330338211064719, 2021.

[31] W. Dörr and J. H. Hendry. Consequential late effects in normal tissues. *Radiotherapy and oncology*, 61(3):223–231, 2001.

[32] P. G. Esposito, R. Castriconi, P. Mangili, A. Fodor, M. Pasetti, N. G. Di Muzio, A. Del Vecchio, and C. Fiorino. Virtual tangential-fields arc therapy (vitat) for whole breast irradiation: Technique optimization and validation. *Physica Medica*, 77:160–168, 2020.

[33] A. Fodor, C. Brombin, P. Mangili, R. Tummineri, M. Pasetti, F. Zerbetto, B. Longobardi, A. S. Galvan, C. L. Deantoni, I. Dell'Oca, et al. Toxicity of hypofractionated whole breast radiotherapy without boost and timescale of late skin responses in a large cohort of early-stage breast cancer patients. *Clinical Breast Cancer*, 22(4):e480–e487, 2022.

[34] K. Gokula, A. Earnest, and L. C. Wong. Meta-analysis of incidence of early lung toxicity in 3-dimensional conformal irradiation of breast carcinomas. *Radiation Oncology*, 8(1):1–12, 2013.

[35] E. B. C. T. C. Group et al. Effects of radiotherapy and of differences in the extent of surgery for early breast cancer on local recurrence and 15-year

survival: an overview of the randomised trials. *The Lancet*, 366(9503):2087–2106, 2005.

[36] E. B. C. T. C. Group et al. Effect of radiotherapy after breast-conserving surgery on 10-year recurrence and 15-year breast cancer death: meta-analysis of individual patient data for 10 801 women in 17 randomised trials. *The Lancet*, 378(9804):1707–1716, 2011.

[37] N. Harbeck. Breast cancer is a systemic disease optimally treated by a multidisciplinary team. *Nature Reviews Disease Primers*, 6(1):1–2, 2020.

[38] J. S. Haviland, J. R. Owen, J. A. Dewar, R. K. Agrawal, J. Barrett, P. J. Barrett-Lee, H. J. Dobbs, P. Hopwood, P. A. Lawton, B. J. Magee, et al. The uk standardisation of breast radiotherapy (start) trials of radiotherapy hypofractionation for treatment of early breast cancer: 10-year follow-up results of two randomised controlled trials. *The lancet oncology*, 14(11):1086–1094, 2013.

[39] J. S. Haviland, J. R. Owen, J. A. Dewar, R. K. Agrawal, J. Barrett, P. J. Barrett-Lee, H. J. Dobbs, P. Hopwood, P. A. Lawton, B. J. Magee, et al. The uk standardisation of breast radiotherapy (start) trials of radiotherapy hypofractionation for treatment of early breast cancer: 10-year follow-up results of two randomised controlled trials. *The lancet oncology*, 14(11):1086–1094, 2013.

[40] T. Hermann, M. Baumann, and W. Dörr. Klinische strahlenbiologie. *Stuttgart, German: Urban & Fischer Verlag*, 2006.

[41] K. M. Higgins and J. R. Wang. State of head and neck surgical oncology research—a review and critical appraisal of landmark studies. *Head & Neck: Journal for the Sciences and Specialties of the Head and Neck*, 30(12):1636–1642, 2008.

[42] X. Huang, O. A. Maguire, J. M. Walker, C. S. Jiang, T. S. Carroll, J.-D. Luo, E. Tonorezos, D. N. Friedman, and P. Cohen. Therapeutic radiation exposure of the abdomen during childhood induces chronic adipose tissue dysfunction. *JCI insight*, 6(21), 2021.

[43] J. Jeba, R. Isiah, J. Subhashini, S. Backianathan, B. Thangakunam, and D. J. Christopher. Radiation pneumonitis after conventional radiotherapy for breast cancer: a prospective study. *Journal of clinical and diagnostic research: JCDR*, 9(7):XC01, 2015.

[44] I. Kindts, A. Laenen, T. Depuydt, and C. Weltens. Tumour bed boost radiotherapy for women after breast-conserving surgery. *Cochrane Database of Systematic Reviews*, (11), 2017.

[45] U. Kraus-Tiefenbacher, A. Sfintizky, G. Welzel, A. Simeonova, E. Sperk, K. Siebenlist, S. Mai, and F. Wenz. Factors of influence on acute skin toxicity of breast cancer patients treated with standard three-dimensional conformal radiotherapy (3d-crt) after breast conserving surgery (bcs). *Radiation oncology*, 7(1):1–9, 2012.

[46] K. Kristensen, S. Pedersen, P. Vestergaard, L. Mosekilde, and B. Richelsen. Hormone replacement therapy affects body composition and leptin differently in obese and non-obese postmenopausal women. *Journal of endocrinology*, 163(1):55–62, 1999.

[47] D. Krug, C. Köder, M. F. Häfner, N. Arians, S. B. Harrabi, S. A. Koerber, T. Forster, I. Schlampp, C. Sohn, J. Heil, et al. Acute toxicity of normofractionated intensity modulated radiotherapy with simultaneous integrated boost compared to three-dimensional conformal radiotherapy with sequential boost in the adjuvant treatment of breast cancer. *Radiation Oncology*, 15(1):1–8, 2020.

[48] G. Lazzari, A. Terlizzi, G. D. V. Scarpati, F. Perri, V. De Chiara, B. Turi, and G. Silvano. Predictive parameters in hypofractionated whole-breast 3d conformal radiotherapy according to the ontario canadian trial. *OncoTargets and therapy*, 10:1835, 2017.

[49] J. Y. Lin, X. Yang, M. Serra, A. H. Miller, K. D. Godette, S. T. Kahn, S. Henry, G. Brown, T. Liu, and M. A. Torres. Full axillary lymph node dissection and increased breast epidermal thickness 1 year after radiation therapy for breast cancer. *Journal of surgical oncology*, 120(8):1397–1403, 2019.

[50] T. Liu, J. Zhou, K. S. Osterman, P. Zhang, S. A. Woodhouse, P. B. Schiff, and G. J. Kutcher. Measurements of radiation-induced skin changes in breast-cancer radiation therapy using ultrasonic imaging. In *2008 International Conference on BioMedical Engineering and Informatics*, volume 2, pages 718–722. IEEE, 2008.

[51] A. Moody, W. Mayles, J. Bliss, R. A'Hern, J. Owen, J. Regan, B. Broad, and J. Yarnold. The influence of breast size on late radiation effects and association with radiotherapy dose inhomogeneity. *Radiotherapy and Oncology*, 33(2):106–112, 1994.

[52] M. Mori, G. Cattaneo, I. Dell'Oca, S. Foti, R. Calandrino, N. Di Muzio, and C. Fiorino. Skin dvhs predict cutaneous toxicity in head and neck cancer patients treated with tomotherapy. *Physica Medica*, 59:133–141, 2019.

[53] M. B. Mukesh, E. Harris, S. Collette, C. E. Coles, H. Bartelink, J. Wilkinson, P. M. Evans, P. Graham, J. Haviland, P. Poortmans, et al. Normal tissue complication probability (ntcp) parameters for breast fibrosis: pooled results from two randomised trials. *Radiotherapy and Oncology*, 108(2):293–298, 2013.

[54] A. Neal, M. Torr, S. Helyer, and J. Yarnold. Correlation of breast dose heterogeneity with breast size using 3d ct planning and dose-volume histograms. *Radiotherapy and oncology*, 34(3):210–218, 1995.

[55] M. Nita and A. Grzybowski. The role of the reactive oxygen species and oxidative stress in the pathomechanism of the age-related ocular diseases and other pathologies of the anterior and posterior eye segments in adults. *Oxidative medicine and cellular longevity*, 2016, 2016.

[56] N. Okonogi, K. Karasawa, Y. Nitta, Y. Mori, K. Murata, M. Wakatsuki, and H. Tsuji. Risk of secondary malignancy after radiotherapy for breast cancer: long-term follow-up of japanese patients with breast cancer. *Breast Cancer Research and Treatment*, 194(3):561–567, 2022.

[57] V. Panettieri, P. Barsoum, M. Westermark, L. Brualla, and I. Lax. Aaa and pbc calculation accuracy in the surface build-up region in tangential beam treatments. phantom and breast case study with the monte carlo code penelope. *Radiotherapy and oncology*, 93(1):94–101, 2009.

[58] G. E. Papadakis, D. Hans, E. G. Rodriguez, P. Vollenweider, G. Waeber, P. Marques-Vidal, and O. Lamy. Menopausal hormone therapy is associated with reduced total and visceral adiposity: the osteolaus cohort. *The Journal of Clinical Endocrinology & Metabolism*, 103(5):1948–1957, 2018.

[59] F. Pastore, M. Conson, V. D'Avino, G. Palma, R. Liuzzi, R. Solla, A. Farella, M. Salvatore, L. Cella, and R. Pacelli. Dose-surface analysis for prediction of severe acute radio-induced skin toxicity in breast cancer patients. *Acta Oncologica*, 55(4):466–473, 2016.

[60] R. Perner. Arm edema in patients treated conservatively for breast cancer; relationship to patient age and axillary node dissection technique. *Int J Radiat Oncol Biol Phys*, 12:2079–2083, 1986.

[61] J.-P. Pignol, I. Olivotto, E. Rakovitch, S. Gardner, K. Sixel, W. Beckham, T. T. T. Vu, P. Truong, I. Ackerman, and L. Paszat. A multicenter randomized

trial of breast intensity-modulated radiation therapy to reduce acute radiation dermatitis. *Journal of Clinical Oncology*, 26(13):2085–2092, 2008.

[62] R. A. Price Jr, S. Koren, I. Veltchev, M. Hossain, M.-H. Lin, T. Galloway, P. Flanagan, J. Haber, and C.-M. Ma. Planning target volume-to-skin proximity for head-and-neck intensity modulated radiation therapy treatment planning. *Practical radiation oncology*, 4(1):e21–e29, 2014.

[63] T. Rancati and C. Fiorino. *Modelling radiotherapy side effects: Practical applications for planning optimisation*. CRC Press, 2019.

[64] J. Reckhow, M. Ben-David, A. Ostrovski, D. Illinsky, J. Goldstein, Z. Symon, and S. Galper. Advantages of continuous positive airway pressure (cpap) in left-sided breast radiation therapy. *International Journal of Radiation Oncology, Biology, Physics*, 102(3):S184, 2018.

[65] L. Rossi, R. Bijman, W. Schillemans, S. Aluwini, C. Cavedon, M. Witte, L. Incrocci, and B. Heijmen. Texture analysis of 3d dose distributions for predictive modelling of toxicity rates in radiotherapy. *Radiotherapy and Oncology*, 129(3):548–553, 2018.

[66] V. Rudat, A. Nour, S. A. Ghaida, and A. Alaradi. Impact of hypofractionation and tangential beam imrt on the acute skin reaction in adjuvant breast cancer radiotherapy. *Radiation Oncology*, 11(1):1–9, 2016.

[67] E. P. Saibishkumar, M. A. MacKenzie, D. Severin, A. Mihai, J. Hanson, H. Daly, G. Fallone, M. B. Parliament, and B. S. Abdulkarim. Skin-sparing radiation using intensity-modulated radiotherapy after conservative surgery in early-stage breast cancer: a planning study. *International Journal of Radiation Oncology* Biology* Physics*, 70(2):485–491, 2008.

[68] A. G. Sanchis, L. B. González, J. L. S. Carazo, J. C. G. Partearroyo, A. E. Martínez, A. V. González, and J. L. L. Torrecilla. Evaluation of acute skin toxicity in breast radiotherapy with a new quantitative approach. *Radiotherapy and Oncology*, 122(1):54–59, 2017.

[69] A. Sardaro, M. F. Petruzzelli, M. P. D'Errico, L. Grimaldi, G. Pili, and M. Portaluri. Radiation-induced cardiac damage in early left breast cancer patients: risk factors, biological mechanisms, radiobiology, and dosimetric constraints. *Radiotherapy and Oncology*, 103(2):133–142, 2012.

[70] P. Seibold, A. Webb, M. E. Aguado-Barrera, D. Azria, C. Bourgier, M. Brengues, E. Briers, R. Bultijnck, P. Calvo-Crespo, A. Carballo, et al.

Requite: a prospective multicentre cohort study of patients undergoing radiotherapy for breast, lung or prostate cancer. *Radiotherapy and Oncology*, 138:59–67, 2019.

[71] C. Shah, Z. Al-Hilli, and F. Vicini. Advances in breast cancer radiotherapy: Implications for current and future practice. *JCO Oncology Practice*, 17(12):697–706, 2021.

[72] M. G. Shah and H. I. Maibach. Estrogen and skin. *American journal of clinical dermatology*, 2(3):143–150, 2001.

[73] C. K. Sites, M. Brochu, E. T. Poehlman, et al. Relationship between hormone replacement therapy use with body fat distribution and insulin sensitivity in obese postmenopausal women. *Metabolism-Clinical and Experimental*, 50(7):835–840, 2001.

[74] B. D. Smith, J. R. Bellon, R. Blitzblau, G. Freedman, B. Haffty, C. Hahn, F. Halberg, K. Hoffman, K. Horst, J. Moran, et al. Radiation therapy for the whole breast: Executive summary of an american society for radiation oncology (astro) evidence-based guideline. *Practical radiation oncology*, 8(3):145–152, 2018.

[75] M. Spałek. Chronic radiation-induced dermatitis: challenges and solutions. *Clinical, cosmetic and investigational dermatology*, 9:473, 2016.

[76] S. Standring. *Gray's anatomy e-book: the anatomical basis of clinical practice*. Elsevier Health Sciences, 2021.

[77] H. Sumino, S. Ichikawa, A. Yoshida, M. Murakami, T. Kanda, H. Mizunuma, T. Sakamaki, and M. Kurabayashi. Effects of hormone replacement therapy on weight, abdominal fat distribution, and lipid levels in japanese postmenopausal women. *International journal of obesity*, 27(9):1044–1051, 2003.

[78] M. A. Torres, X. Yang, S. Noreen, H. Chen, T. Han, S. Henry, D. Mister, F. Andic, Q. Long, and T. Liu. The impact of axillary lymph node surgery on breast skin thickening during and after radiation therapy for breast cancer. *International Journal of Radiation Oncology* Biology* Physics*, 95(2):590–596, 2016.

[79] T. S. Trialists' Group. The uk standardisation of breast radiotherapy (start) trial b of radiotherapy hypofractionation for treatment of early breast cancer: a randomised trial. *The Lancet*, 371(9618):1098–1107, 2008.

[80] I. Turesson and H. D. Thames. Repair capacity and kinetics of human skin during fractionated radiotherapy: erythema, desquamation, and telangiectasia after 3 and 5 year's follow-up. *Radiotherapy and Oncology*, 15(2):169–188, 1989.

[81] J. Van Dongen, H. Bartelink, I. Fentiman, T. Lerut, F. Mignolet, G. Olthuis, E. Van der Schueren, R. Sylvester, D. Tong, J. Winter, et al. Factors influencing local relapse and survival and results of salvage treatment after breast-conserving therapy in operable breast cancer: Eortc trial 10801, breast conservation compared with mastectomy in tnm stage i and ii breast cancer. *European journal of cancer*, 28(4-5):801–805, 1992.

[82] K. R. Voong, K. McSpadden, C. C. Pinnix, F. Shihadeh, V. Reed, M. R. Salehpour, I. Arzu, H. Wang, D. Hodgson, J. Garcia, et al. Dosimetric advantages of a "butterfly" technique for intensity-modulated radiation therapy for young female patients with mediastinal hodgkin's lymphoma. *Radiation Oncology*, 9(1):1–9, 2014.

[83] J. Werbrouck, K. De Ruyck, F. Duprez, L. Veldeman, K. Claes, M. Van Eijkeren, T. Boterberg, P. Willems, A. Vral, W. De Neve, et al. Acute normal tissue reactions in head-and-neck cancer patients treated with imrt: influence of dose and association with genetic polymorphisms in dna dsb repair genes. *International Journal of Radiation Oncology* Biology* Physics*, 73(4):1187–1195, 2009.

[84] A. G. Wernicke, M. Shamis, K. K. Sidhu, B. C. Turner, Y. Goltser, I. Khan, P. J. Christos, and L. T. Komarnicky-Kocher. Complication rates in patients with negatve axillary nodes 10-years after local breast radiotherapy following either sentinel lymph node dissection or axillary clearance. *American journal of clinical oncology*, 36(1):12, 2013.

[85] T. J. Whelan, J.-P. Pignol, M. N. Levine, J. A. Julian, R. MacKenzie, S. Parpia, W. Shelley, L. Grimard, J. Bowen, H. Lukka, et al. Long-term results of hypofractionated radiation therapy for breast cancer. *New England Journal of Medicine*, 362(6):513–520, 2010.

[86] H. R. Withers, J. M. Taylor, and B. Maciejewski. Treatment volume and tissue tolerance. *International Journal of Radiation Oncology* Biology* Physics*, 14(4):751–759, 1988.

[87] T. Yanagi, T. Kamada, H. Tsuji, R. Imai, I. Serizawa, and H. Tsujii. Dose–volume histogram and dose–surface histogram analysis for skin reactions to

carbon ion radiotherapy for bone and soft tissue sarcoma. *Radiotherapy and Oncology*, 95(1):60–65, 2010.

[88] E. Yoshida, H. Chen, M. Torres, W. Curran, and T. Liu. Spectrophotometer and ultrasound evaluation of late toxicity following breast-cancer radiotherapy. *Medical Physics*, 38(10):5747–5755, 2011.

[89] D. A. Young-Afat, M. L. Gregorowitsch, D. H. van den Bongard, I. Burgmans, C. C. van der Pol, A. J. Witkamp, R. M. Bijlsma, R. Koelemij, E. J. Schoenmaeckers, Y. Jonasse, et al. Breast edema following breast-conserving surgery and radiotherapy: patient-reported prevalence, determinants, and effect on health-related quality of life. *JNCI cancer spectrum*, 3(2):pkz011, 2019.

[90] Q. Zhang, J. Liu, N. Ao, H. Yu, Y. Peng, L. Ou, and S. Zhang. Secondary cancer risk after radiation therapy for breast cancer with different radiotherapy techniques. *Scientific reports*, 10(1):1–12, 2020.